

OAK RIDGE NATIONAL LABORATORY

operated by

UNION CARBIDE CORPORATION

for the

U.S. ATOMIC ENERGY COMMISSION



ORNL - TM - 479 *Self*

COPY NO. - 56

DATE - Feb. 28, 1963

SOME APPLICATIONS OF MAGNETOHYDRODYNAMICS IN CONFINED VORTEX FLOWS

J. J. Keyes, Jr.

ABSTRACT

The possibility that magnetohydrodynamic (MHD) interactions might be utilized advantageously for control and/or generation of high velocity confined vortex flows is considered in order to delineate the situations of greatest potential application and to suggest directions which future analytical and experimental work should take. The cases surveyed in most detail are (1) the hydrodynamically driven, MHD stabilized free vortex, analyzed previously by Chang, and (2) the MHD driven and stabilized vortex, stability criteria for which are developed in this report as an extension of Chang's analysis. In both cases idealized conditions of inviscid, incompressible, perfectly conducting flow are assumed. Preliminary numerical results suggest that, within the limitations imposed by the theoretical assumptions, stabilization of a hydrodynamically driven free vortex against turbulent breakdown due to small perturbations may be possible, using an axial magnetic field which, though relatively high, may be attainable in practice. Application to a H^+ plasma core fission reactor is discussed.

Analysis of vortices driven by interaction of applied axial magnetic and radial electric fields has indicated that, while it is in principle possible to obtain stabilization under certain conditions discussed in this report, the electrical energy input required to maintain the radial electric current flow may be prohibitively high for plasma reactor application.

Analysis of the Hall effect for the case of a viscous, incompressible MHD driven vortex with finite electrical conductivity has indicated that neglect of the Hall current term in the generalized Ohm's law expression will probably introduce negligible error for conditions of practical interest. Appreciable simplification of all subsequent MHD analysis is therefore possible. Recommendations for additional theoretical studies and for the initiation of an experimental program are discussed.

NOTICE

This document contains information of a preliminary nature and was prepared primarily for internal use at the Oak Ridge National Laboratory. It is subject to revision or correction and therefore does not represent a final report. The information is not to be abstracted, reprinted or otherwise given public dissemination without the approval of the ORNL patent branch, Legal and Information Control Department.

LEGAL NOTICE

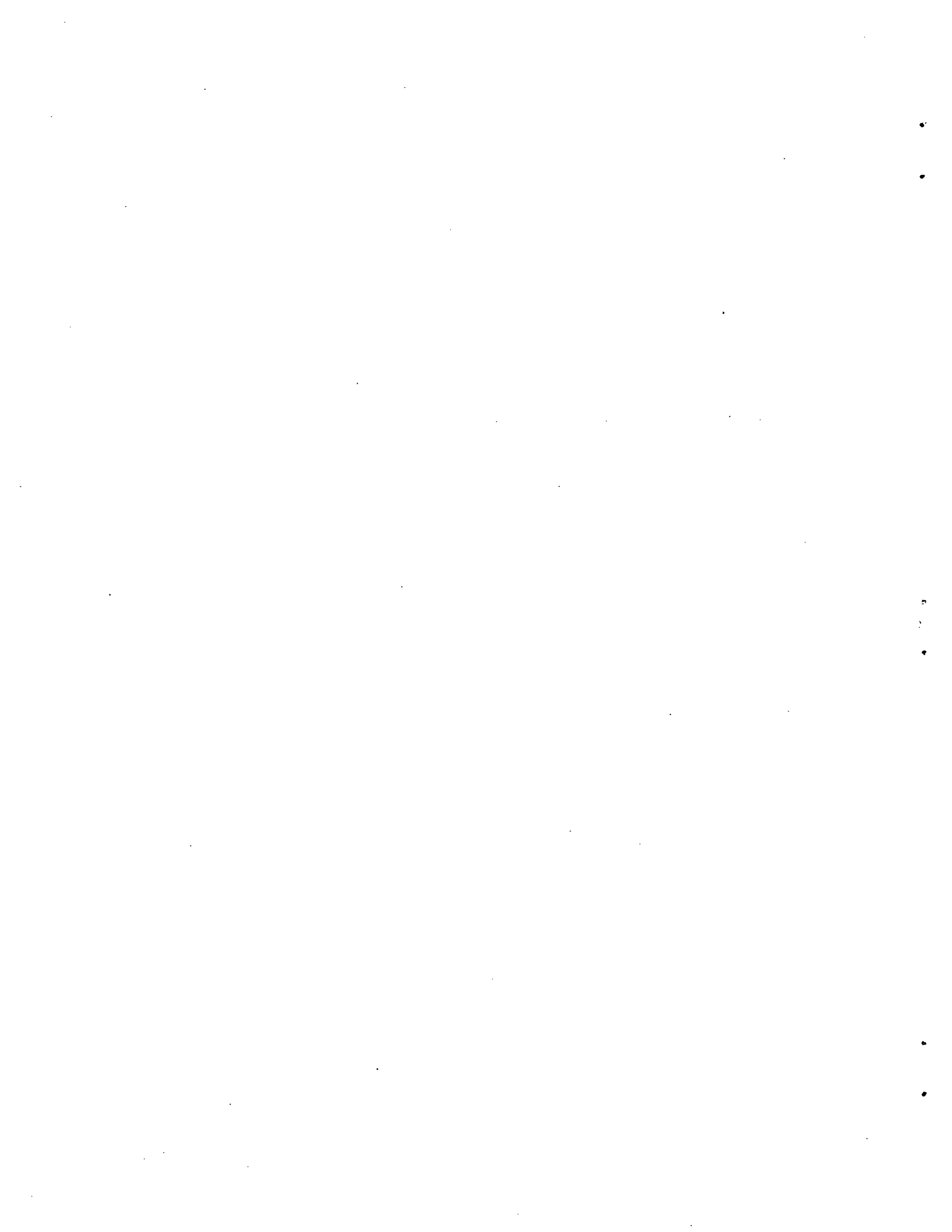
This report was prepared as an account of Government sponsored work. Neither the United States, nor the Commission, nor any person acting on behalf of the Commission:

- A. Makes any warranty or representation, expressed or implied, with respect to the accuracy, completeness, or usefulness of the information contained in this report, or that the use of any information, apparatus, method, or process disclosed in this report may not infringe privately owned rights; or
- B. Assumes any liabilities with respect to the use of, or for damages resulting from the use of any information, apparatus, method, or process disclosed in this report.

As used in the above, "person acting on behalf of the Commission" includes any employee or contractor of the Commission, or employee of such contractor, to the extent that such employee or contractor of the Commission, or employee of such contractor prepares, disseminates, or provides access to, any information pursuant to his employment or contract with the Commission, or his employment with such contractor.

CONTENTS

	<u>Page</u>
Introduction	5
Literature Review	9
Summary of Steady-State Magnetohydrodynamic Solutions	12
Summary of MHD Stabilization Solutions	18
A. Hydrodynamically Driven Vortexes With No Radial Mass Flow	18
B. Magnetohydrodynamically Driven Vortexes With Very Low Radial Mass Flow	18
Numerical Examples	22
A. Hydrodynamically Driven Hydrogen Plasma Vortex Employing MHD Stabilization	22
B. Magnetohydrodynamically Driven Hydrogen Plasma Vortex Employing MHD Stabilization	27
Conclusion	30
Acknowledgment	31
Appendix I - Analysis of the Hall Effect for a Magnetohydro- dynamically Driven Vortex With No Radial Mass Flow	32
Appendix II - Extension of T. S. Chang's Stability Analysis to the Case of a Magnetohydrodynamically Driven Vortex With an Applied Radial Electric Field	38
References	46
Nomenclature	48



SOME APPLICATIONS OF MAGNETOHYDRODYNAMICS IN CONFINED VORTEX FLOWS

J. J. Keyes, Jr.

INTRODUCTION

Consideration of the unique fluid mechanical properties of vortex-type flows has stimulated interest in the application of these flows to certain advanced concepts in power generation and propulsion. The magnetohydrodynamic (MHD) vortex power generator, described by Donaldson,¹ Lewellan,^{2,3} Knoernschild,⁴ and others, for example, utilizes a plasma in vortex flow interacting with an axial magnetic field to generate a radial electric field. The cavity gaseous fission reactor concept described by Kerrebrock and Megreblian⁵ depends on a vortex-type velocity field for containment of the fissionable material. Rosa⁶ has proposed coupling a cavity reactor to an MHD generator.

These applications of vortex flow require, among other things, that the flow field be characterized by a low turbulence level, hence low viscous dissipation, so that the power required for sustaining the vortex will be small compared with the power generated by the device. In addition, applications which involve gas-phase separation (e.g., propulsion) require low turbulence levels to minimize eddy mixing and thus to maintain a high degree of separation.

It should be emphasized that these devices must operate at very high tangential velocities for high efficiency and thus the tangential Reynolds moduli are very high. The desired velocity field approximates that of constant angular momentum (free vortex), a field which Chandrasekhar⁷ and Chang⁸ have shown to be fundamentally unstable with respect to small disturbances. Furthermore, since these are internal flows over concave surfaces, the boundary layers are unstable due to three-dimensional disturbances of the type considered by Göertler.⁹ Finally, if the vortices are jet driven, the high velocity jets themselves are an additional source of turbulent fluctuations. These factors (high Reynolds moduli combined with basic hydrodynamic instability and turbulent driving sources) lead to the conclusion that the flow fields will be turbulent particularly near the

periphery. Experimental confirmation of this conclusion is reported by Keyes and Dial,¹⁰ Donaldson,¹ and Rosenzweig.¹¹ In fact, the turbulence levels near the periphery may be sufficiently high as to seriously challenge the feasibility of these devices.

Attempts to reduce the turbulence level in vortex flows by purely hydrodynamic means have met with only partial success. One approach is the vortex matrix suggested by Kerrebrock and studied by Rosenzweig.¹¹ A technique under investigation at the Oak Ridge National Laboratory involves generation of the vortex by flow through a uniformly porous wall with pores oriented nearly tangentially; a sort of artificial rotating wall is thus produced in which adjacent jets may ride on each other with minimum interaction in the boundary layer. These studies should be continued.

An alternative method which can, in principle, produce a significant stabilizing influence involves the interaction between the velocity field in an electrically conducting medium and a suitably oriented magnetic field, making use of the Lorentz force which might be looked upon in this application as a restoring body force exerted on a fluid volume element when it is displaced from its position of equilibrium. In two-dimensional vortex flow, a uniform axial magnetic field will function to induce stability over the entire flow field. Since the devices of interest will operate at temperatures sufficiently high to sustain ionization in the gas either thermally or by seeding, the possibility of magnetohydrodynamic stabilization must not be overlooked. For example, Chang⁸ has shown that a uniform axial magnetic field is in principle capable of completely stabilizing an inviscid, perfectly conducting pure vortex flow against small perturbations without altering the mean flow distribution. In the case of jet-driven vortices, however, the jets themselves can introduce forced boundary oscillations and hence perturbations which may prevent complete stabilization, although partial stabilization may be effected. Instability of flow against concave walls is another source of instability. These effects must be considered further.

Lewellan² has proposed generating the vortex magnetohydrodynamically by interaction of an axial magnetic field with a radial electric field,

for example, to produce a tangential Lorentz body force (inverse of the MHD generator). For generation of strong vortices by this technique, it can be shown that the turbulence level must be low. Elimination of the driving jets eliminates the source of forced oscillations, but there is still the source of instability due to flow over a concave surface. It is shown in a later section of this report that Chang's stability analysis can be extended to the case of an MHD driven vortex with small radial current flow, and it is concluded that MHD forces may also be able to stabilize the flow in this case.

In addition to the turbulence problem in vortex flows, there is also the serious problem of flow in the end wall boundary layers which short-circuits radial flow away from the interior of the vortex cavity. In MHD applications, there is a corresponding shorting of the electric field at the end walls. One potential advantage of the application of MHD interactions in connection with vortex flows is the possibility that magnetic and/or electric fields can be utilized to control the inward radial boundary-layer flow. This application is not considered here, however, but should be the subject of further study.

It is the purpose of this report to consider in a general way the application of MHD to the problem of vortex stabilization against turbulent breakdown for the separate cases of hydrodynamically and magneto-hydrodynamically driven vortices. The basic stability analysis of Chang presented in ref. 8 is employed, with an extension to the case of small radial current flow. The steady-state (stationary) solutions for the velocity profiles corresponding to the various cases of interest (see Table 1) are obtained to the zeroth order using the approximate technique described by Lewellan in ref. 1. In addition, the effect of inclusion of the Hall current term in the generalized Ohm's law expression is discussed in this report. Sample calculations for a reference case of practical interest are included to give an indication of orders of magnitude of the important variables, and a proposal is made for continued analytical work and for initiation of an experimental program.

Table 1. Summary of Magnetohydrodynamic Cases Considered

Condition or Property	Assumption					
Density, ρ	Constant [Incompressible Flow]					
Viscosity, μ	0 [Inviscid Flow]			Constant ($\neq 0$) [Viscous Flow]		
Electrical Conductivity, σ	Infinite		Finite	Finite		
Radial Velocity, Q_r	0	$0 < Q_r < \epsilon^*$	$\ll Q_0$	0	$\ll Q_0$	
Hall Coefficient, h	0	0	0	0	$\neq 0$ [$\partial B_r / \partial z \cong 0$]	0
Applied Radial Electric Current Density, J_0	0	$\neq 0$	$\neq 0$	$\neq 0$	$\neq 0$	$\neq 0$
	Type of Solution Obtained					
	Steady-State & Stabilization Criterion, Eqs. (3) & (4)	Steady-State & Stabilization Criterion, Eqs. (bp) & (bq)	Steady-State, ² Eq. (an)	Steady-State, Eq. (ai)	Steady-State, Eq. (ah)	Steady-State, ² Eq. (2)

* ϵ is an arbitrarily small, positive, real quantity.

LITERATURE REVIEW

The stabilizing influence of a magnetic field on linear flow of an incompressible fluid between parallel walls was examined by Stuart¹² and by Lock¹³ for the case of a transverse field. Both authors derived criteria for neutral stability in terms of the Hartmann modulus, N_H (defined on page 25); it was found, for example, that the stabilizing effect of a transverse magnetic field is far greater than that of a longitudinal one. Hartmann and Lazarus¹⁴ observed experimentally that the pressure drop required to produce a given flow of mercury in a rectangular channel was decreased by a moderate magnetic field, in spite of the induction drag, and postulated that this was due to reduction in turbulence by the field. It was also observed that the presence of a magnetic field tended to extend the laminar flow range. Murgatroyd¹⁵ observed that the transition Reynolds modulus was proportional to N_H . Harris¹⁶ presents a detailed analysis of MHD channel flows.

Chandrasekhar⁷ analyzed the effect of an axial magnetic field on the stability of Couette flow of a viscous, incompressible fluid between rotating cylinders. By assuming the cylinders to rotate in the same direction (the inner cylinder the faster) and by assuming the gap between the cylinders to be small compared with their radii, Chandrasekhar obtained a relation between the ratio by which the angular velocities have to be increased to produce instability as a function of the Hartmann modulus based on the gap width. For example, to produce instability in mercury with a field of 1000 gauss and with a 1-cm gap, the cylinders must rotate ten times as fast as in the absence of the field. Thus the field exerts a very significant stabilizing influence.

The first successful experiments to ascertain the effects of an axial magnetic field on the stability of Couette flow are those of Donnelly and Ozima.¹⁷ The experiments amply confirm the theoretical predictions of Chandrasekhar.

The stability criterion developed by Chang⁸ for inviscid, incompressible, perfectly conducting vortex flow relates the peripheral Alfvén number, A_P ($\equiv Q_P / \sqrt{B_0^2 / \rho \mu_0}$), for stabilization to the radius ratio, κ .*

* See Nomenclature, page 48.

The relationship is plotted in Fig. 1. It is concluded that, for this simplified case, the magnetic field required for stabilization varies in proportion to the tangential peripheral velocity, Q_p , the square root of the fluid density, ρ , and transcendently with the inner and outer radii of the vortex boundaries. Estimates of the magnetic field required for stabilizing a 6000°K , 100 atm H^+ plasma may be found on page 25 of this report.

Donaldson¹ has considered briefly the effect of a magnetic field on the properties of turbulent vortex motion, and has concluded that the turbulence may "begin to differ from its usual form" when the Hartmann modulus based on an "effective shearing length" of the vortex chamber approaches 200. It is shown on page 25 that this conclusion is compatible, for the H^+ plasma, with an estimate based on Chang's theory.

Boedeker and Covert¹⁸ measured the effect of a transverse magnetic field on the helical flow of hydrochloric acid solution and found measurable MHD interaction with the primary (mean) and secondary flow structure only when the Reynolds and Hartmann moduli were approximately equal, and at least of the order of unity. On the other hand, Murgatroyd¹⁵ found, for mercury flowing in a parallel wall channel, that the Reynolds modulus had to exceed the Hartmann modulus by a factor of at least 225 for turbulence to occur, suggesting that magnetic effects for this case are significant at much higher relative values of Reynolds modulus than observed by Boedeker and Covert for helical flow. It is apparent that additional analytical and experimental work is needed in this field. Boedeker and Covert conclude, significantly, that the continuum MHD assumption is valid for electrolytes in the absence of large gradients.

MHD driven vortexes are discussed by Lewellan,² who obtained zeroth order steady-state solutions for two general cases, involving axial current-radial magnetic field and radial current-axial magnetic field. It was assumed, in order to obtain the boundary conditions, that the inner and outer cylinders are porous, with the outer cylinder rotating. Fluid was assumed to be introduced uniformly through the outer cylinder and removed uniformly through the inner cylinder. The assumption made in the present analysis is that both cylinders are fixed; the method of solution for the steady-state

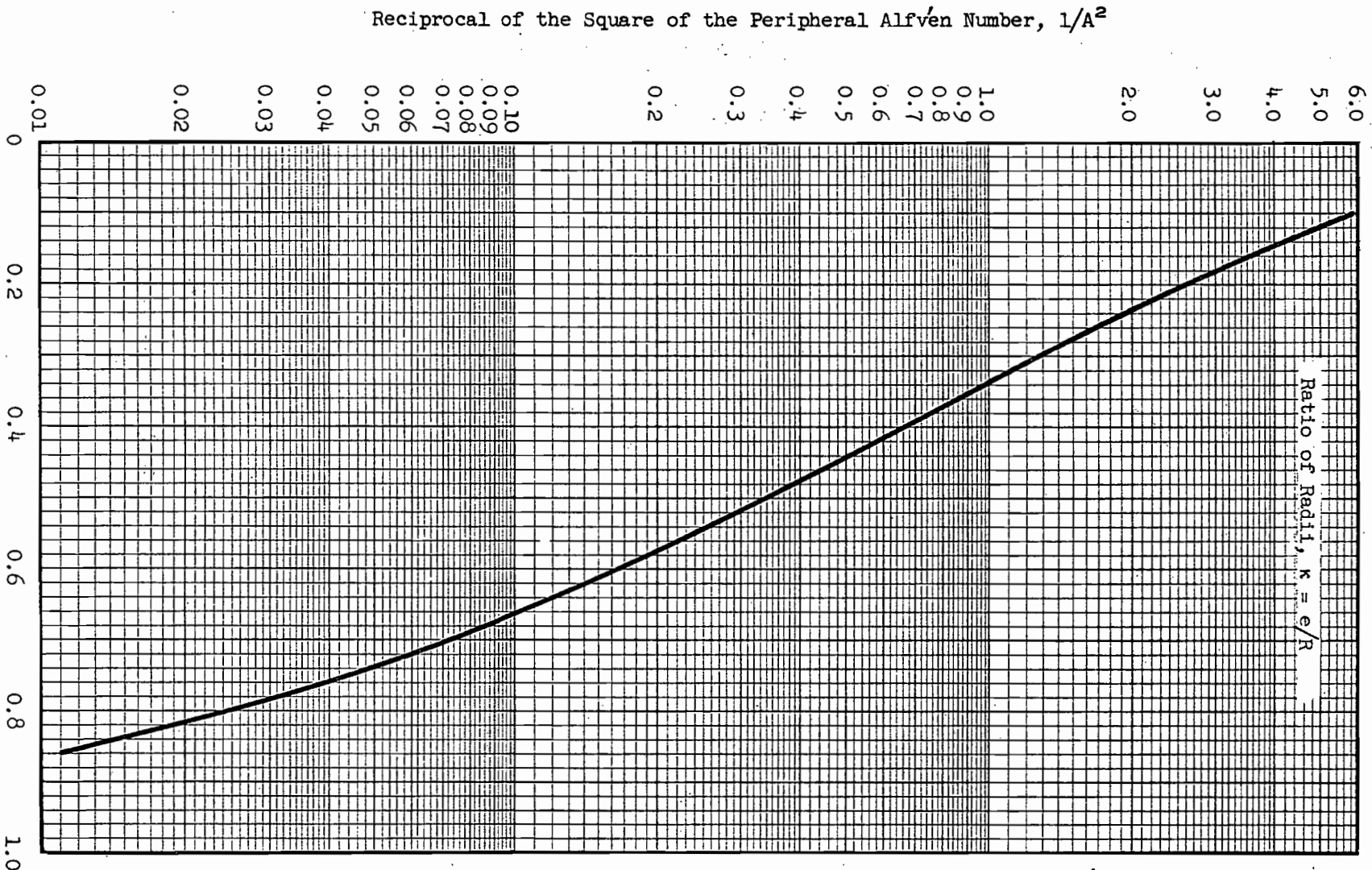


Fig. 1. Dependence of the Reciprocal of the Square of the Peripheral Alfvén Number to Insure Vortex Stability on the Ratio of the Radii of the Cylinders Containing the Vortex.

UNCLASSIFIED
ORNL-IR-DWG. 75879

cases is essentially the same as that employed by Lewellan with the inclusion of the Hall effect in one of the cases analyzed (Table 1).

SUMMARY OF STEADY-STATE MAGNETOHYDRODYNAMIC SOLUTIONS

The basic steady-state assumptions common to the analyses of all cases considered here and summarized in Table 1 are:

1. The medium is a homogeneous neutral continuum contained between two coaxial cylinders. The outer cylinder is assumed fixed; the inner cylinder may be rotated.
2. The fluid density is constant.
3. The flow is axisymmetric, two-dimensional, nonturbulent.
4. The electric field is axisymmetric, with $E_\theta = 0$.
5. The square of the radial velocity is negligible compared with the square of the tangential velocity.
6. The radial magnetic Reynolds modulus, $N_M (= \mu_0 \sigma Q_r r)$, is sufficiently small that induced electric and magnetic fields can be neglected in comparison with the applied electric and magnetic fields (zeroth order approximation).
7. The applied magnetic field is uniform and in the axial direction; the applied electric field is radial.

The special cases considered and the additional conditions and assumptions employed are listed in Table 1. Detailed analyses of the cases may be found in Appendices I and II.

A. MHD Driven Vortexes

Conditions: Finite conductivity, viscous flow, constant viscosity ($\neq 0$), zero radial mass flow.

1. Hall Effect Included

Many MHD solutions neglect the Hall current by taking $h = 0$ in Eq. (h), Appendix I. In order to develop a quantitative criterion for neglect

of the Hall effect, the analysis detailed in Appendix I and summarized here is included:

The effective (Hall) electrical conductivity is

$$\sigma' = \frac{\sigma}{1 + h^2 \sigma^2 B_0^2}, \quad (y)^*$$

where the Hall coefficient, $h = 1/ne' = 1.037 \times 10^{-4}$ (W/a₀).** Note that the Hall effect results in a decrease in the effective electrical conductivity with increase in magnetic field strength.

The approximate criterion for neglect of the Hall effect in vortex flow, as derived in Appendix I (subject to the assumptions listed on page 12), is:

$$\frac{1}{\mu_0 \sigma' h R J_0} \gg |\ln \kappa| \quad (ae)$$

With $J_0 = I_0 / 20 \pi R$ (I_0 is the applied current, amp/cm), Eq. (ae) becomes:

$$\frac{20 \pi}{\mu_0 \sigma' h I_0} \gg |\ln \kappa| \quad (1)$$

Values of h , $1 - \sigma'/\sigma$, and $20 \pi / \mu_0 \sigma' h I_0$ are summarized in Table 2 for some specific cases and conditions of interest. For comparison, $|\ln \kappa| \leq 2.3$ for $\kappa \geq 0.1$.

* Equations with alphabetic designations are taken from the Appendices.

** CGS-EM units are used in this report except where specifically noted.

Table 2. Hall Effect in Vortex Flow

Case	h	$\frac{\sigma' - \sigma}{\sigma}$ ($B_0 = 10^5$ gauss)	$20 \pi / \mu_0 \sigma h I_0$, ($I_0 = 100$ amp/cm)
(1) Hg (20°C)	7.6×10^{-4}	1×10^{-6}	6×10^6
(2) NaK (Eutectic, 20°C)	4.2×10^{-3}	2×10^{-4}	4×10^5
(3) NH ₄ Cl (Saturated, aqueous solution, 60°C)	2×10^{-3}	4×10^{-14}	2×10^{10}
(4) H ⁺ Plasma (Seeded, 6000°K, 100 atm)	5×10^{-1}	1×10^{-6}	5×10^7

Maximum anticipated values of B_0 and I_0 are used in the calculations as indicated. It is concluded that the Hall effect is negligible for these cases of interest. For example, σ' differs from σ by at most 0.02% [Case (2)]; furthermore, Eq. (1) is satisfied since

$$\frac{20 \pi / \mu_0 \sigma h I_0}{|\ln \kappa|} \geq 2 \times 10^5 \quad [\text{Case (2)}]$$

for $\kappa \geq 0.1$. The Hall effect will be neglected in all subsequent analyses without further verification.*

2. Hall Effect Neglected

The relationship for the steady-state tangential velocity, Q_θ , subject to the boundary conditions $Q_\theta = 0$ at $r' = \kappa$ and at $r' = 1$ is given in Appendix I:

$$Q_\theta = - \frac{J_0 B_0 R^2}{2 \mu} \left(\frac{1}{\kappa^2 - 1} \right) \left[\left(r' - \frac{1}{r'} \right) \kappa^2 \ln \kappa + (r' \ln r') (1 - \kappa^2) \right], \quad (\text{ai})$$

$$(r' = r/R, \kappa = e/R) \quad .$$

*The Hall effect might be significant for a very high temperature, low pressure plasma, a case which is not considered here.

This relationship is plotted in dimensionless form in Fig. 2 for $\kappa = 0.1$ and 0.25. Since J_0 is the applied radial current density at the periphery, which can be expressed as $J_0 = I_0/20 \pi R$, it follows that Q_θ varies directly with the product $I_0 B_0 R$, inversely with μ , and transcendently with κ and r' . Decreasing κ increases the tangential velocity at every radial position.

B. MHD Driven Vortexes

Conditions: Finite conductivity, viscous flow, constant viscosity ($\neq 0$), non-zero radial mass flow but with the restriction

$$Q_r \ll Q_\theta .$$

The following equation for Q_θ (subject to the boundary conditions for case A.2) may be obtained from Lewellan's analysis:²

$$Q_\theta = - \frac{\pi J_0 B_0 R^2}{m} \left\{ \left(\frac{\kappa^2 - 1}{\kappa^{N+2} - 1} \right) \left[(r')^{N+1} - \frac{1}{r'} \right] + \left(\frac{1}{r'} - r' \right) \right\} , \quad (2)$$

where $N \equiv - \frac{m}{2 \pi \mu}$, the radial Reynolds modulus.

(m is the radial mass flow rate per unit length of vortex tube.)

For this case, Q_θ varies directly with $I_0 B_0 R$, inversely with m , and transcendently with N , κ , and r' . For $N = -\infty$ ($\mu = 0$), Eq. (2) reduces to:

$$Q_\theta = - \frac{\pi J_0 B_0 R^2}{m} \left[\frac{1}{r'} - r' \right] . \quad \text{(an)} \quad [\text{see Appendix II}]$$

From Fig. 3, a graph of Eq. (2), it is seen that the curves for $N = -100$, $\kappa = 0.1$, and for $N = -\infty$, $\kappa = 0.1$, are identical for $r' > 0.125$ (i.e., over most of the radius range). Since, for mass flow rates of interest in the vortex reactor application, N will be -100 or less provided the flow field is not turbulent, Eq. (an) can be used as a very good approximation for Q_θ in a stabilized system. Furthermore, it should be pointed out that the influence of κ is not significant (except, of course, for $r' \approx \kappa$) so long as $N \geq -10$. The effect of increasing κ from 0.1 to 0.25 for $N = -4$ (turbulent flow) is shown by the two lower curves in Fig. 3.

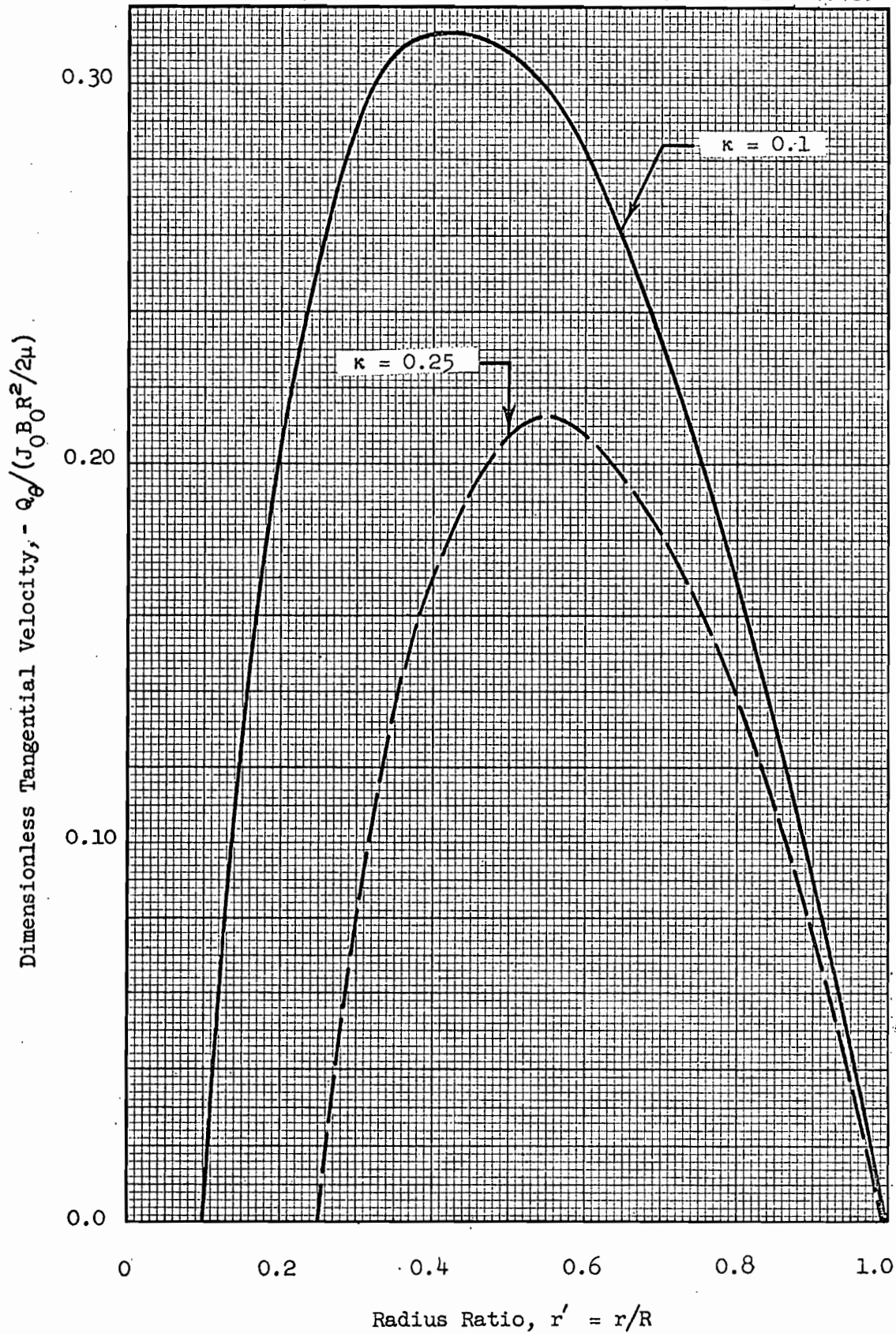
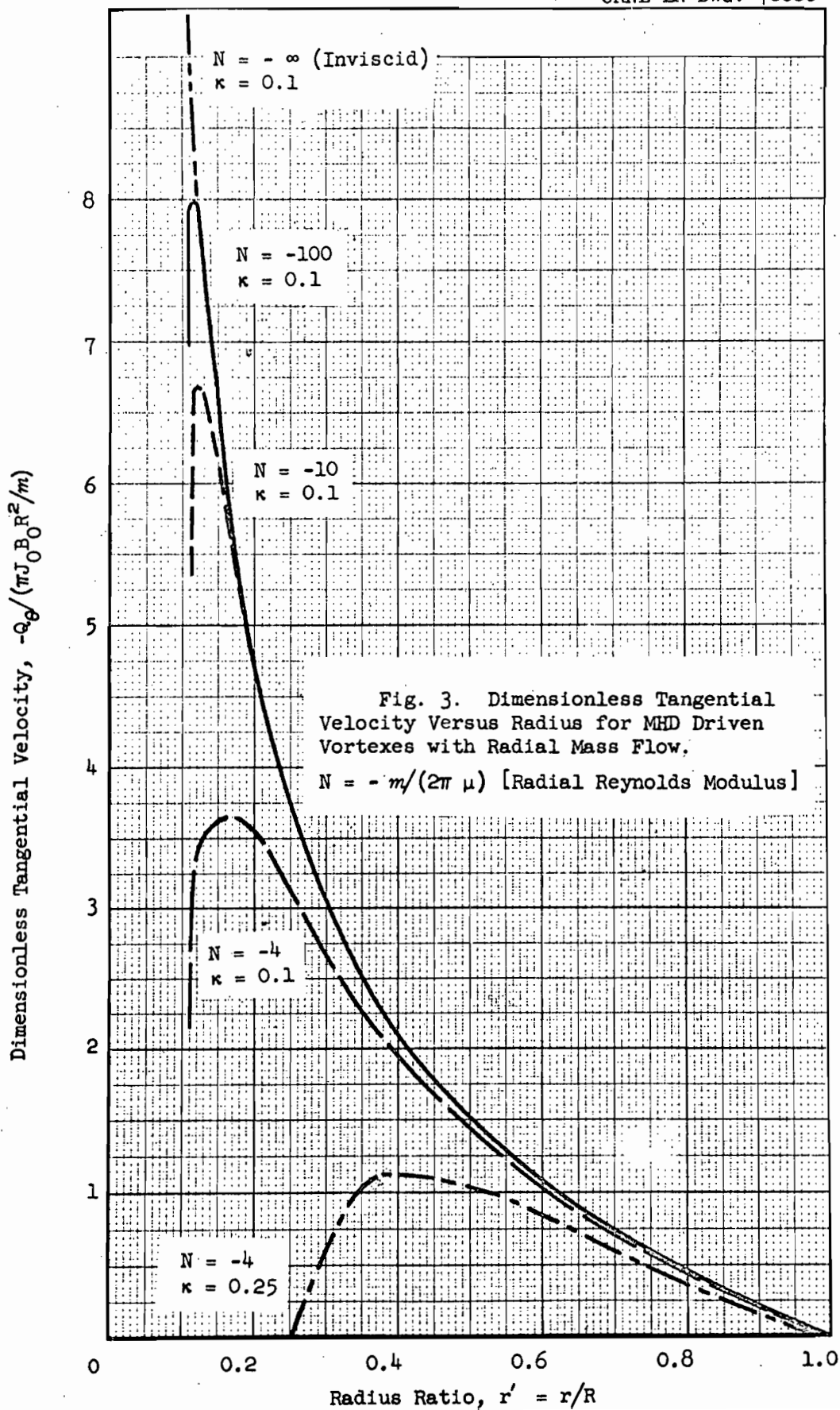


Fig. 2. Dimensionless Tangential Velocity Versus Radius for an MHD Driven Viscous Vortex with No Radial Mass Flow.



SUMMARY OF MHD STABILIZATION SOLUTIONS

The basic assumptions, in addition to those listed on page 12, are:

- (a) Inviscid flow, $\mu = 0$.
- (b) Infinite electrical conductivity, $\sigma = \infty$.
- (c) No Hall effect, $h = 0$.
- (d) Small perturbations.

A. Hydrodynamically Driven Vortexes With No Radial Mass Flow

$$J_0 = 0, \quad Q_r = 0$$

This is the case analyzed by Chang in ref. 8. The approximate stability criterion is:

$$\frac{1}{A_p^2} \geq \beta(\kappa) \equiv \frac{\kappa \int_{\kappa}^1 \frac{y_{r'}^2}{r'^3} dr'}{\int_{\kappa}^1 r' \left(\frac{dy_{r'}}{dr'} + \frac{y_{r'}}{r'} \right)^2 dr'}, \quad (3)$$

where

$$A_p \equiv Q_p / \sqrt{B_0^2 / \rho \mu_0}$$

is the peripheral Alfvén modulus. Chang assumes

$$y_{r'} = y_{r'}^0 \sin \left[\frac{\pi (r' - \kappa)}{1 - \kappa} \right] \quad (4a)$$

$1/A_p^2$ is plotted versus κ in Fig. 1.

The approximate magnetic field strength required for stability is [from Eq. (3) and the definition of A_p]:

$$B_0 \geq Q_p \sqrt{\mu_0 \rho \beta(\kappa)} \quad (4)$$

B. Magnetohydrodynamically Driven Vortexes With Very Low Radial Mass Flow

Chang's analysis has been extended to include the case in which the vortex is driven by the $\underline{J} \times \underline{B}$ tangential body force resulting from the

interaction of an applied radial electric current and an applied axial magnetic field. The following additional assumptions and restrictions are necessary for this case (as discussed in Appendix II):

- (a) Inviscid flow, $\mu = 0$.
 - (b) Infinite electrical conductivity, $\sigma = \infty$.
 - (c) $J_0 = \text{const.} (\neq 0)$.
 - (d) $0 < Q_r < \epsilon$.
 - (e) $|B_\theta| = \mu_0 J_0 R \frac{z}{r} = \frac{I_0 z}{5 r} \ll B_0$,
- for any z/r , especially $(z/r)_{\text{max}} = L/e$.

A sufficient stability criterion for an MHD driven vortex subject to the above assumptions is obtained in Appendix II:*

$$\frac{1}{A_e^2} = \frac{4 \kappa^2}{(1 - \kappa^2)^2} \phi(\kappa) \quad , \quad (\text{bp})$$

where

$$\phi(\kappa) \equiv \left\{ \frac{\int_{\kappa}^1 \frac{y_{r'}^2 (r'^2 - 1)^2 dr'}{r'^3}}{\int_{\kappa}^1 r' \left(\frac{dy_{r'}}{dr'} + \frac{y_{r'}}{r'} \right)^2 dr'} \right\}$$

and $y_{r'}$ is given by Eq. (bo). A_e is the Alfvén modulus based on Q_e , the maximum tangential velocity which occurs at the inner reference radius, $r' = \kappa = e/R$:

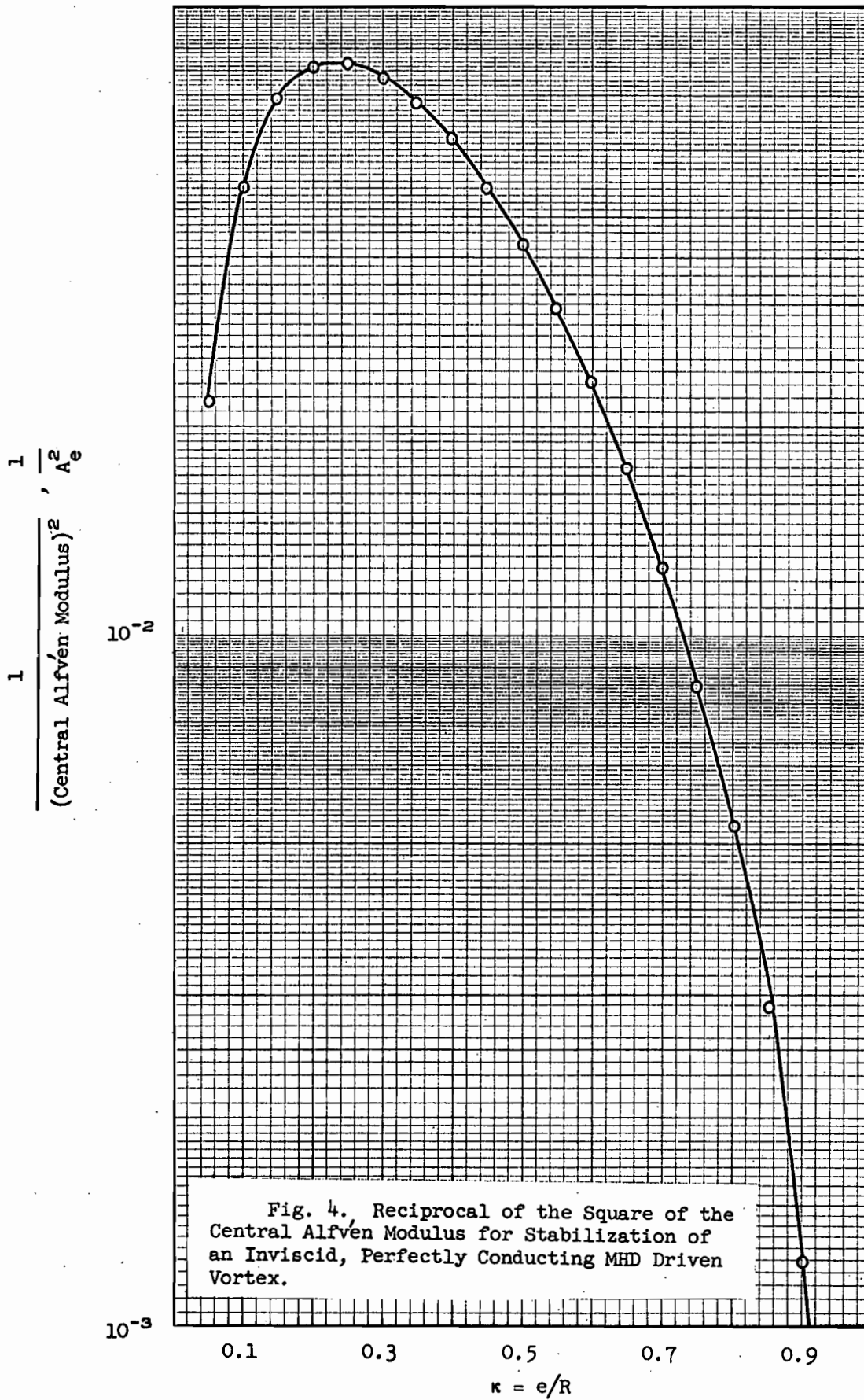
$$A_e \equiv \frac{|Q_e|}{\sqrt{B_0^2 / \rho \mu_0}} \quad . \quad (5)$$

Figures 4 and 5 graph the dependence of $1/A_e^2$ and $\phi(\kappa)$ on κ .

From the definition of A_e [Eq. (5)], the stability criterion can be written explicitly:

* Appendix II, pages 45 and 46, should be referred to for a discussion of more general stability criteria.

Unclassified
ORNL-LR-DWG 79790



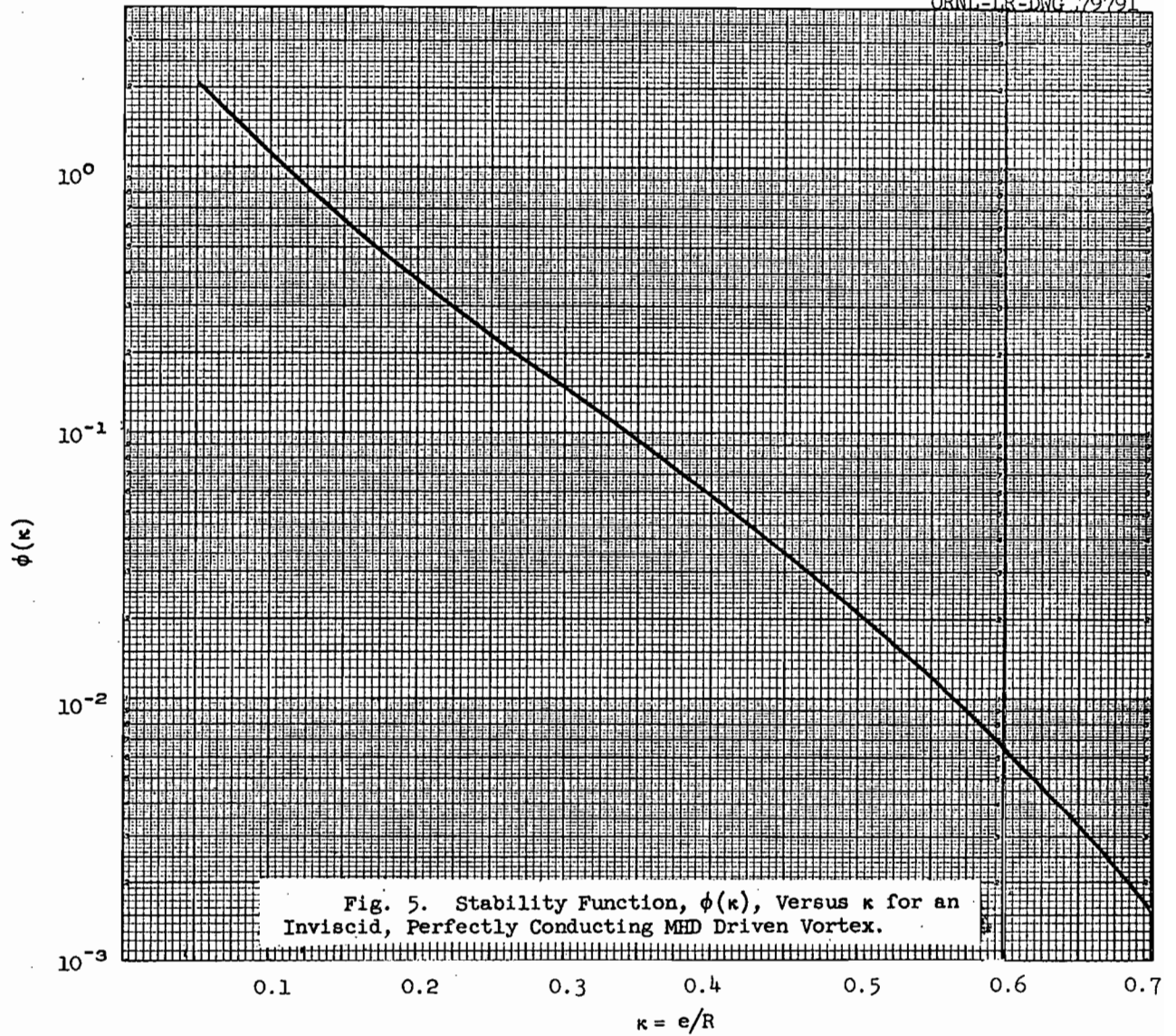
Unclassified
ORNL-IR-DWG 79791

Fig. 5. Stability Function, $\phi(\kappa)$, Versus κ for an Inviscid, Perfectly Conducting MHD Driven Vortex.

$$\frac{B_0}{|Q_e|} = 2 \left(\frac{\kappa}{1 - \kappa^2} \right) \sqrt{\mu_0 \rho \phi(\kappa)} \quad (\text{bq})$$

Hence, the magnetic field required for stabilizing the vortex varies directly with the tangential velocity and the square root of the density, and transcendently with the radius ratio. Note the similarity between this expression and that applicable to the original case, Eq. (4). For the hydrodynamically driven vortex, the peripheral tangential velocity, Q_p , is independent of B_0 , but for the MHD vortex, Q_e and B_0 are related by Eq. (bn):

$$Q_e = - \frac{I_0 B_0 R}{20 m} \left(\frac{1 - \kappa^2}{\kappa} \right) \quad (\text{bn})$$

An alternate but equivalent stability criterion involving the applied electric current per unit length, I_0 , is given in Appendix II as:

$$\frac{I_0 R}{m} = \frac{10}{\sqrt{\mu_0 \rho \phi(\kappa)}} \quad (\text{br})$$

Figures 6 and 7 are graphs of the relationships expressed by Eqs. (bq) and (br) for three reference densities corresponding to Hg and NaK at 70°C and to H^+ at 6000°K, 100 atm, representing conditions which might prevail respectively in experimental studies and in the ultimate application to a plasma reactor.

NUMERICAL EXAMPLES

A. Hydrodynamically Driven Hydrogen Plasma Vortex Employing MHD Stabilization

Consider, for reference, a hypothetical plasma core reactor utilizing vortex containment and operating under the following assumed conditions:

H^+ plasma at 6000°K, 100 atm pressure, having an effective density $\rho = 2.2 \times 10^{-4}$ g/cc (neglecting fuel concentration) is the working fluid. Based on previous studies,¹⁹ it is estimated that a peripheral tangential

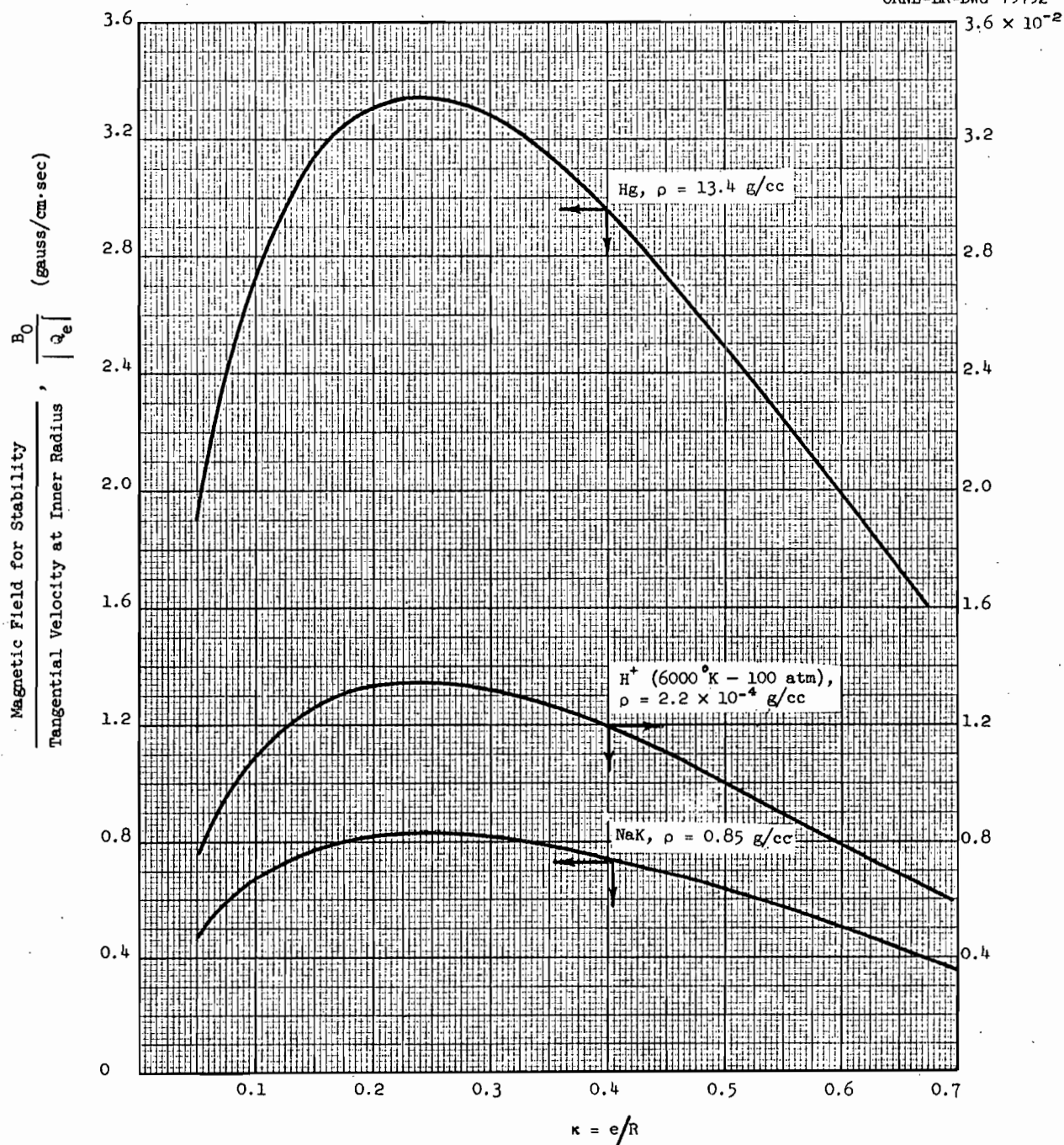


Fig. 6. Magnetic Field Required for Stabilization of an Inviscid, Perfectly Conducting MHD Driven Vortex for Three Reference Densities.

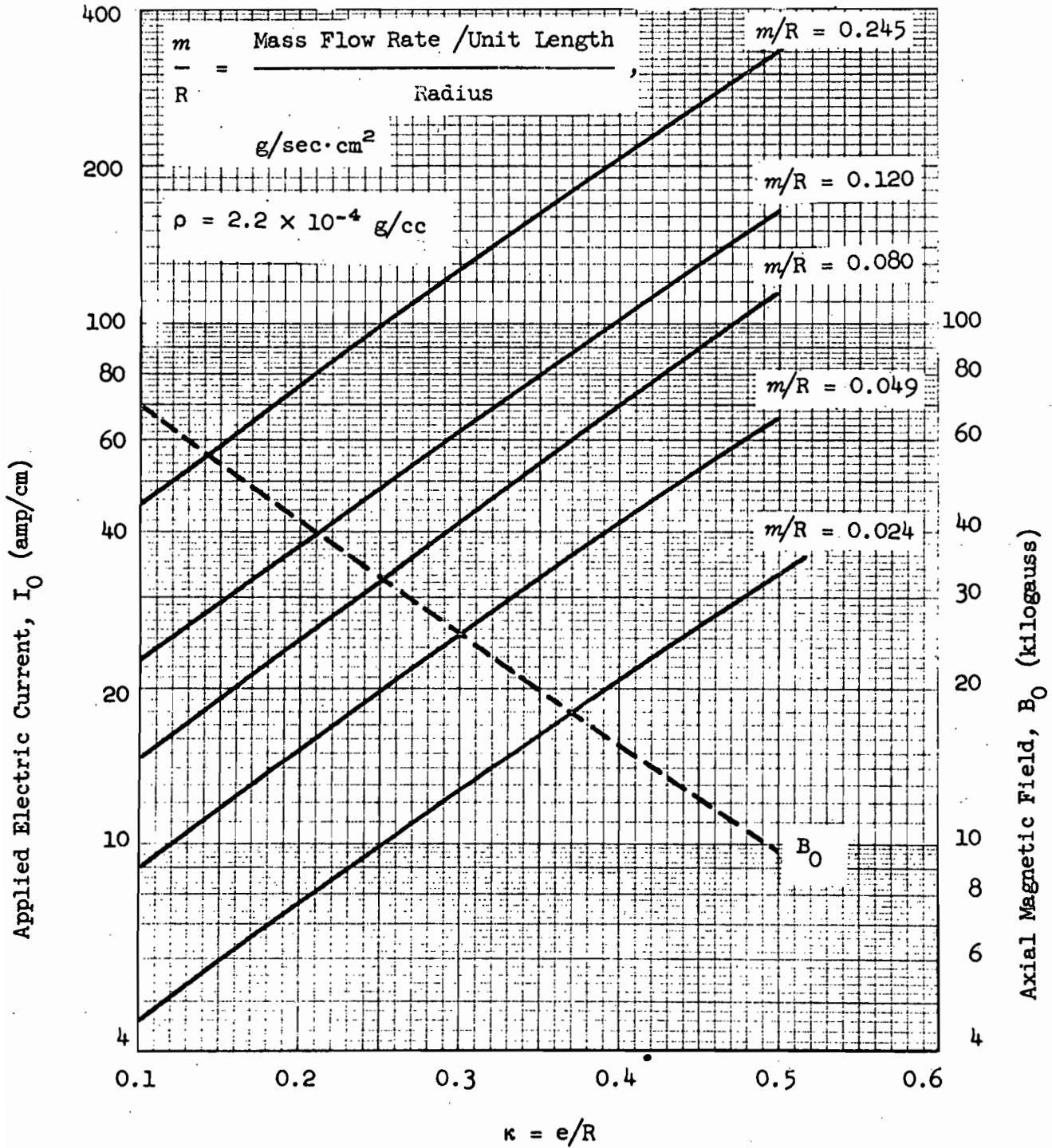
UNCLASSIFIED
ORNL-LR-DWG. 78878

Fig. 7. Applied Electric Current and Magnetic Field Required to Generate and Stabilize Inviscid H^+ (6000°K, 100 atm) Vortexes with Tangential Mach Number = 0.35 at $r' = 0.8$.

Mach number of at least 0.5 may be required for satisfactory containment of the nuclear fuel in the gas core reactor concept. For H at 6000°K, the sonic velocity is about 8×10^5 cm/sec so that Q_p may have to be of the order of 4×10^5 cm/sec for satisfactory performance.

A gross estimate of the axial magnetic field required to stabilize a free vortex ($1/r$ characteristic) under these conditions can be made using Eq. (5) by assuming inviscid flow, negligible radial mass flow, constant density and temperature, and "effectively" infinite electrical conductivity. Since these conditions are artificial for the present case, it must be emphasized that the calculated results are useful only as initial "guesses" in lieu of a more realistic analysis.

Figure 8 is a plot of the axial magnetic field required to stabilize a vortex having the properties and characteristics just discussed. Note that increasing the ratio κ of exit radius to tube radius decreases the magnetic field from about 51,500 gauss at $\kappa = 0.1$ to 12,000 gauss at $\kappa = 0.5$.

By the criterion of Donaldson (as discussed on page 10),

$$N_H = \left(\sqrt{\sigma/\mu} \right) B_0 L \geq 200 \quad (6)$$

if the magnetic field is to have an appreciable effect on the turbulence. Taking $\sigma = 2$ mho/cm (2×10^{-9} emu/cm) for a seeded H, H^+ plasma, $\mu = 6 \times 10^{-4}$ poise, and L (the effective shearing length) = 5 cm, $B_0 = 22,000$ gauss, a result which is (perhaps coincidentally) within the range of values predicted by the theory of Chang.

Assuming that an axial magnetic field of the order of 30,000 gauss will be sufficient to stabilize a free vortex for the reactor application, the question arises as to whether generation of this high a field is practical for the intended use. The question can best be considered in terms of the additional weight and power required to maintain the field. For example, a typical gaseous core nuclear rocket engine might consist of 12,000 1.2-in.-diam vortex tubes, 14 ft in length, based on Case No. 1 of the analysis by Kerrebrock and Meghreblian.⁵ Such a reactor would have a power output of perhaps 40,000 thermal mw, and generate a thrust of 4×10^6 lb, with a reactor weight of 1.2×10^5 lb.

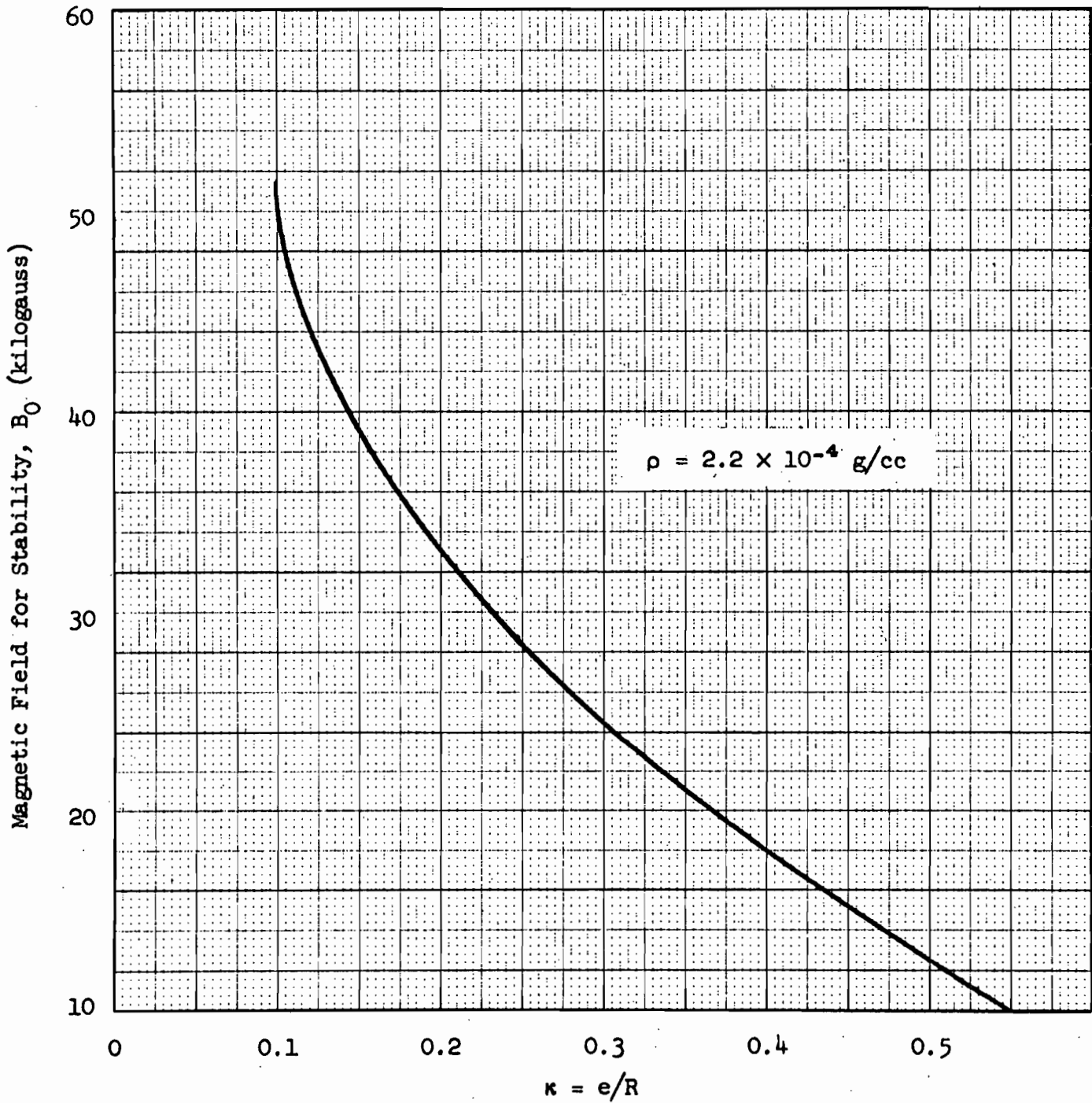


Fig. 8. Axial Magnetic Field Strength Required to Stabilize an Hydrodynamically Driven Free H^+ Vortex having a Peripheral Tangential Velocity, $Q_p = 4 \times 10^5 \text{ cm/sec}$.

A rough estimate of the power required to generate 30,000 gauss (by means of a solenoidal coil) over an area enclosing 12,000 tubes of 1.2-in. diameter on 1.8-in. centers indicates that, if cryogenic cooling is used so that the resistance of copper is reduced to 10% of its 20°C value,* the field can be generated with the total expenditure of perhaps 20 m_w of electrical power. Assuming 30% conversion efficiency, the power required to maintain this field is only about 0.2% of the power output of the reactor. The coil and necessary electrical supply may weigh perhaps 150,000 lb.** Thus, a major penalty associated with the use of the magnetic field for stabilization is the decrease in available thrust-to-weight ratio. It is possible that an MHD electrical generator driven by a side stream of heated hydrogen from the plasma core reactor, as discussed by Lewellan and Grabowsky,³ might provide the necessary electrical power with appreciably less weight penalty. A more detailed system analysis must, of course, be carried out to determine optimum operating conditions, minimum gross weight, etc. This is probably not justified until a more realistic analysis is completed and some experimental studies carried out.

B. Magnetohydrodynamically Driven Hydrogen Plasma Vortex Employing MHD Stabilization

Stabilization of an hydrodynamically driven vortex may be more difficult than the preliminary calculations for Case A indicate, due to the destabilizing influence of boundary perturbations induced by the driving jets which was not considered in the analysis. This source of boundary perturbations can be eliminated by driving the vortex magnetohydrodynamically, using an applied radial electric field in addition to the axial magnetic field (as discussed on pages 14 and 15 and in ref. 2). As a matter of fact, referring to Fig. 3, it is possible to attain higher tangential velocities in the interior of the vortex field for the same peripheral tangential velocity with magnetohydrodynamically as compared with hydrodynamically driven vortices. For example, an MHD driven vortex having a

* Using cold H₂ propellant.

** Assuming 5 lb/kwe based on the analysis of a 20 mwe turboelectric power plant (ref. 20) and assuming that some weight reduction is possible for a reactor with unprotected radiator and very short time operation. Alternatively, the use of a superconductor might greatly lower the power requirement for the magnet.

tangential Mach number of 0.35 at $r' = 0.8$ is equivalent so far as the gaseous reactor application is concerned to a jet driven vortex ($\sim 1/r$ velocity profile) having a tangential peripheral Mach number of 0.5 as assumed for Case A.

Figure 7 is a graph of the applied electric current, I_0 , and of the applied axial magnetic field, B_0 , required to generate and stabilize an inviscid hydrogen (H^+) vortex at $6000^\circ K$, 100 atm (conditions of Case A) having a tangential Mach number at $r' = 0.8$ of 0.35 ($Q_\theta = 2.8 \times 10^5$ cm/sec at $r' = 0.8$). This graph is obtained from Fig. 6 and Eqs. (an), (bn), and (br). Note that I_0 depends on m/R , the ratio of radial mass flow rate per unit length to tube radius. For Kerrebrock and Meghreblian's Case 4, $m = 0.18$ g/sec·cm and $R = 1.55$ cm; hence, $m/R = 0.12$. From Fig. 7 for $\kappa = 0.2$, $I_0 = 37$ amp/cm, $B_0 = 40,000$ gauss; for $\kappa = 0.35$, $I_0 = 78$ amp/cm, $B_0 = 20,000$ gauss.

To the electrical power required for the magnetic field must be added the power represented by the flow of electric current, I_0 , through the seeded plasma of assumed average conductivity, 2 mho/cm. The radial voltage drop, ΔV , across the vortex tube can be calculated from the Ohm's law [Eq. (u)], Appendix I, with $h = 0$:

$$J_r = \sigma (E_r + Q_\theta B_0) \quad , \quad (u)$$

$$\Delta V = R \int_{\kappa}^1 E_r(r') dr' = R \int_{\kappa}^1 \left(\frac{J_r(r')}{\sigma} - Q_\theta(r') B_0 \right) dr' .$$

Since $Q_\theta(r') = -\frac{I_0 B_0 R}{20 m} \left(\frac{1}{r'} - r' \right)$ from Eq. (an),

$$\begin{aligned} \Delta V \text{ (volts)} &= \frac{I_0}{2\pi} \left\{ \frac{\ln(1/\kappa)}{\sigma} + \frac{10^{-9} \pi B_0^2 R^2}{m} \left[\ln(1/\kappa) - \frac{1 - \kappa^2}{2} \right] \right\} \\ &= \Delta V \text{ (OHMIC)} + \Delta V \text{ (drive)} . \end{aligned} \quad (7)$$

For $\kappa = 0.2$, $I_0 = 37$ amp/cm, $B_0 = 40,000$ gauss, $m = 0.18$ g/sec·cm, and $R = 1.55$ cm, $\Delta V = 4.7 + 410.0 = 414.7$ volts.

$$\begin{aligned} \therefore \text{Radial power input} &= I_0 \Delta V = 173 \text{ w/cm (ohmic)} + 15,000 \text{ w/cm (drive)} \\ &= 15,173 \text{ w/cm.} \end{aligned}$$

For $\kappa = 0.35$, $I_0 = 78 \text{ amp/cm}$, $B_0 = 20,000 \text{ gauss}$, $m = 0.18 \text{ g/sec.cm}$, and $R = 155 \text{ cm}$, $\Delta V = 6.5 + 121.0 = 127.5 \text{ volts}$.

$$\begin{aligned} \therefore \text{Radial power input} &= 470 \text{ w/cm (ohmic)} + 9500 \text{ w/cm (drive)} \\ &= 10,000 \text{ w/cm.} \end{aligned}$$

For the case under consideration with 12,000 tubes 14 ft in length, the total radial power input amounts to about $5 \times 10^{10} \text{ w}$, or approximately 3000 times the power required to maintain the magnetic field.

For comparison, a hydrodynamically (jet) driven vortex having a peripheral tangential Mach number of 0.5 would require a power input equivalent to perhaps 2000 w/cm to generate the vortex if stabilized so as to operate under viscous flow conditions and neglecting effects of magnetically induced drag. Thus, the power input required to drive the vortex by MHD may be appreciably greater than for the jet driven vortex.* Furthermore, the MHD driven vortex requires electrical energy from a converter whereas the hydrodynamically driven vortex may obtain the required kinetic energy (or equivalent enthalpy) directly from the thermal energy output of the reactor. An additional problem with the MHD driven vortex is the requirement that there be a central ionized core much more electrically conducting than the outer regions of the plasma to serve essentially as an "electrode" for establishing the radial electric field. For these reasons, the magnetohydrodynamically driven vortex looks at the present less promising than the hydrodynamically driven vortex provided the later can be stabilized against turbulent breakdown in the manner previously considered.

* The additional power for the MHD case results primarily from the fact that the tangential velocity profile is much steeper than for the hydrodynamic case; hence, velocities generated near the center of the vortex are higher, even though the peripheral velocity is lower.

CONCLUSION

This cursory discussion of some magnetohydrodynamic effects in vortex flows is intended primarily as a basis for recommendation of additional, more general analytical work, and of the initiation of an exploratory experimental program. The numerical results indicate that, for the idealized conditions assumed in the analyses, stabilization of a hydrodynamically driven free vortex may be feasible for the plasma reactor application; the concept of a magnetohydrodynamically driven and stabilized vortex, while of much fundamental interest, may not be feasible for this application due, among other causes, to the requirement of very large electrical energy input.

The limitations of the present theory are many, as discussed herein; obvious extensions most urgently needed are:

1. inclusion of the effect of viscous dissipation,
2. inclusion of the effects of finite electrical conductivity,
3. consideration of the influence on stabilization of forced boundary oscillations arising from driving jets and from three-dimensional boundary-layer flow phenomena,
4. consideration of the influence of three-dimensional flow in the interior of the vortex field,
5. inclusion of compressibility effects.

In addition, analysis of the influence of magnetic and electric fields on the wall boundary-layer flows is needed to ascertain whether MHD control of these "short-circuiting" flows is possible, and to suggest ways in which this control might be achieved. The possibility of "overstabilization" with resultant magnetohydrodynamically induced oscillations should also be considered. As the analysis progresses, extension of the "zeroth" order approximation for the case of small magnetic Reynolds modulus considered thus far to higher orders of approximation should be attempted.

The initial phase of a proposed experimental investigation will probably involve flow visualization studies of turbulent transition and secondary flow phenomena in jet driven tubes of the uniform multi-pored type

discussed on page 6 to minimize the effect of jet-induced boundary oscillations. An electrolyte such as NH_4Cl in aqueous solution ($\sigma \approx 1$ mho/cm) may be used as the working fluid (based on the conclusions of ref. 7) for ease of handling and to simulate the conductivity of a low temperature, seeded plasma. A 62,500 gauss magnetic field is available at ORNL. This experiment points up the immediate need for extension of the theory to the case of finite electrical conductivity and nonzero viscosity.

ACKNOWLEDGMENT

The author wishes to acknowledge the helpful assistance of Tien S. Chang in his review of Appendix II. The author is also grateful to R. E. Funderlich, Central Data Processing, for computational assistance, and to Dolores Eden for preparation of the final manuscript.

APPENDIX I

Analysis of the Hall Effect for a Magneto-hydrodynamically
Driven Vortex with no Radial Mass Flow

For steady-state, two-dimensional vortex flow, the basic magneto-hydrodynamic equations in accord with assumptions 1, 2, and 3 (page 12) are:

Continuity: $Q_{i,i} = 0$. (a)*

Motion: $\rho Q_j Q_{i,j} + p_{,i} = \mu Q_{i,jj} + \epsilon_{i,k} J_j B_k$. (b)

Maxwell's Equations: $\epsilon_{ijk} E_{k,j} = 0$, (c)

$\epsilon_{ijk} B_{k,j} = \mu_0 J_i$, (d)

$E_{i,i} = 0$, (e)

$B_{i,i} = 0$, (f)

Charge Continuity: $J_{i,i} = 0$. (g)

Ohm's Law: $J_i = \sigma (E_i + \epsilon_{ijk} Q_j B_k - h \epsilon_{ijk} J_j B_k)$, (h)

$h = 1/ne'$ (Hall coefficient) . (i)

In cylindrical coordinates (with the additional assumptions: 4, 5, 6, 7, page 12) these equations become:

Continuity: $\frac{\partial(r Q_r)}{\partial r} = 0$ ($r Q_r = \text{const.}$) . (j)

Motion: $-\rho \frac{Q_\theta^2}{r} + \frac{\partial p}{\partial r} = \frac{J_\theta B_0}{r}$, (k)

where

$B_0 \equiv$ applied axial magnetic field.

* Index notation as discussed by Chang²¹ is employed.

$$Q_r \frac{\partial Q_\theta}{\partial r} + \frac{Q_\theta Q_r}{r} = \frac{\mu}{\rho} \left\{ \frac{1}{r} \left[\frac{\partial}{\partial r} \left(r \frac{\partial Q_\theta}{\partial r} \right) \right] - \frac{Q_\theta}{r^2} \right\} - \frac{J_r B_0}{\rho} \quad (l)$$

$$\frac{\partial p}{\partial z} = B_\theta J_r \quad (m)$$

Maxwell's Equations: $\frac{\partial E_z}{\partial r} = \frac{\partial E_r}{\partial z} \quad , \quad (n)$

$$\frac{\partial B_\theta}{\partial z} = -\mu_0 J_r \quad , \quad (o)$$

$$\frac{\partial B_r}{\partial z} - \frac{\partial B_z^*}{\partial r} = \mu_0 J_\theta \quad , \quad (p)$$

where $B_z^* \equiv$ induced axial magnetic field.

$$\frac{\partial B_\theta}{\partial r} + \frac{B_\theta}{r} = \mu_0 J_z \quad , \quad (q)$$

$$\frac{1}{r} \frac{\partial(r E_r)}{\partial r} + \frac{\partial E_z}{\partial z} = 0 \quad , \quad (r)$$

$$\frac{1}{r} \frac{\partial(r B_r)}{\partial r} + \frac{\partial B_z}{\partial z} = 0 \quad . \quad (s)$$

Charge Continuity: $\frac{1}{r} \frac{\partial(r J_r)}{\partial r} + \frac{\partial J_z}{\partial z} = 0 \quad . \quad (t)$

(Note that these equations are not all independent.)

Ohm's Law: $J_r = \sigma(E_r + Q_\theta B_0 - h J_\theta B_0) \quad , \quad (u)$

$$J_\theta = \sigma(-Q_r B_0 + h J_r B_0) \quad , \quad (v)$$

$$J_z = \sigma(-B_r Q_\theta - h J_r B_\theta) \quad . \quad (w)$$

Equations (j) through (w) might be called the "zeroth order" MHD approximation equations.

In order to develop an approximate steady-state criterion for evaluating the importance of the Hall current term in the Ohm's law [Eqs. (u), (v), (w)], the following simple illustrative case is treated [see Table 1]:

$$\mu = \text{constant},$$

$$\sigma = \text{finite},$$

$$Q_r = 0 \quad .$$

Equation (l) therefore becomes:

$$J_r B_0 = \mu \left\{ \frac{1}{r} \left[\frac{\partial \left(r \frac{\partial Q_\theta}{\partial r} \right)}{\partial r} \right] - \frac{Q_\theta}{r^2} \right\} \quad . \quad (l')$$

Equation (v) becomes:

$$J_\theta = \sigma(h J_r B_0) \quad . \quad (v')$$

Combining Eqs. (u) and (v'):

$$J_r = \sigma' (E_r + Q_\theta B_0) \quad , \quad (x)$$

where σ' is the "effective" (Hall) electrical conductivity defined by:

$$\sigma' \equiv \frac{\sigma}{1 + h^2 \sigma^2 B_0^2} \quad . \quad (y)$$

Differentiating Eq. (w):

$$\frac{\partial J_z}{\partial z} = \sigma \left(-Q_\theta \frac{\partial B_r}{\partial z} - h J_r \frac{\partial B_\theta}{\partial z} - h B_\theta \frac{\partial J_r}{\partial z} \right) \quad . \quad (z)$$

Combining Eqs. (z), (t), and (o):

$$-\frac{1}{r} \frac{\partial(r J_r)}{\partial r} = \sigma \left(-Q_\theta \frac{\partial B_r}{\partial z} + \mu_0 h J_r^2 \right) .$$

[Note that $h B_\theta (\partial J_r / \partial z)$ is of second order compared with $\mu_0 h J_r^2$ and has therefore been neglected.]

To the zeroth order, B_r itself is small, and if $\partial B_r / \partial z$ is assumed negligibly small in the above equation:*

$$\frac{1}{r} \frac{d(r J_r)}{dr} = -\mu_0 \sigma h J_r^2 . \quad (\text{aa})$$

The solution of Eq. (aa) subjected to the boundary condition that $J_r = J_0$ at $r = R$ is:

$$J_r = \frac{1}{\mu_0 \sigma h r \left(\frac{1}{\mu_0 \sigma h R J_0} + \ln \frac{r}{R} \right)} . \quad (\text{ab})$$

A criterion for determination of the importance of the Hall term is apparent from Eq. (ab). If

$$\frac{1}{\mu_0 \sigma h R J_0} \gg \left| \ln \frac{r}{R} \right| , \quad (\text{ac})$$

then

$$J_r = \frac{J_0 R}{r} , \quad (\text{ad})$$

which is the zeroth order approximation for J_r with the Hall effect neglected. Since the largest value of $\left| \ln \frac{r}{R} \right|$ is $|\ln \kappa|$ where $\kappa = \frac{e}{R}$, the approximate criterion for neglecting the Hall effect in vortex flow is:

$$\frac{1}{\mu_0 \sigma h r J_0} \gg \left| \ln \kappa \right| . \quad (\text{ae})$$

*This is the weakest assumption employed in the analysis of this case. It is justified because the analysis here is intended only as an approximation for the Hall effect in vortex flow.

It is seen that the criterion depends on σ , R , J_0 , and κ in addition to the Hall coefficient, h .

To find Q_θ , Eqs. (l') and (ab) are combined:

$$\frac{1}{r} \left[\frac{d \left(r \frac{dQ_\theta}{dr} \right)}{dr} \right] - \frac{Q_\theta}{r^2} = \frac{B_0}{\mu_0 \sigma h \mu} \left[\frac{1}{r \ln(H' r)} \right], \quad (\text{af})$$

where

$$H' = \frac{1}{R} \exp \left(\frac{1}{\mu_0 \sigma h r J_0} \right). \quad (\text{ag})$$

Taking as boundary conditions $Q_\theta = 0$ at $\left\{ \begin{array}{l} r = e \\ r = R \end{array} \right\}$ (i.e., fixed concentric bounding cylinders), Eq. (af) has the solution:

$$Q_\theta = \frac{B_0}{2 \mu_0 \sigma h \mu H'} \left[C_1 H' r + \frac{C_2}{H' r} + \left\{ \left(H' r - \frac{1}{H' r} \right) \ln(\ln H' r) - \frac{1}{H' r} \left[2 \ln(H' r) + F(H' r) \right] \right\} \right], \quad (\text{ah})$$

where

$$F(H' r) \equiv \sum_{n=2}^{\infty} \frac{2^n \ln^n(H' r)}{n \cdot n!},$$

$$C_1 = \left(\kappa - \frac{1}{\kappa} \right) \left\{ \frac{\ln \left(\frac{\ln H' e}{\ln H' R} \right)}{(H')^2 R e} + \frac{1}{(H')^2 R e} \left[2 \ln \kappa + F(H' e) - F(H' R) \right] + \frac{1}{\kappa} \ln(\ln H' R) - \kappa \ln(\ln H' e) \right\},$$

$$C_2 = \left(\frac{1}{\kappa} - \kappa \right) \left[(H')^2 \operatorname{Re} \ln \left(\frac{\ln H' R}{\ln H' e} \right) - \kappa \left\{ \ln \left[(H' R)^2 \ln H' R \right] \right\} + \right. \\ \left. + \frac{1}{\kappa} \left\{ \ln \left[(H' e) \ln (H' e) \right] \right\} - \kappa F(H' R) + \frac{1}{\kappa} F(H' e) \right] .$$

Hall Effect Negligible

When the criterion stated in Eq. (ae) is satisfied, Eq. (ah) reduces, after considerable manipulation, to

$$Q_\theta = - \frac{J_0 B_0 R^2}{2 \mu} \left(\frac{1}{\kappa^2 - 1} \right) \left[\left(r' - \frac{1}{r'} \right) \kappa^2 \ln \kappa + (r' \ln r') (1 - \kappa^2) \right] , (ai)$$

where

$$r' = \frac{r}{R} .$$

APPENDIX II

Extension of T. S. Chang's Stability Analysis to the Case of a Magneto-hydrodynamically Driven Vortex with an Applied Radial Electric Field

The basic assumptions made by Chang⁸ in addition to those listed on page 12 are:

- (a) $\mu = 0$,
- (b) $\sigma = \infty$,
- (c) $J_0 = 0$ (no applied radial electric current),
- (d) $Q_r = 0$ (no mean radial flow),
- (e) Hall current effect neglected ($h = 0$).

For this case, Chang obtained the following steady-state solutions:

$$Q_r = \frac{K_1}{r} , \quad (\text{aj})$$

$$Q_\theta = \frac{K_2}{r} , \quad (\text{ak})$$

$$Q_z = K_3 . \quad (\text{al})$$

For the case of interest here, assumptions (a), (b), and (e) will be retained. Assumption (c) is replaced by

$$(c') \quad J_0 = \text{const.} \neq 0 ,$$

and (d) by

$$(d') \quad 0 < Q_r < \epsilon ,$$

where ϵ is arbitrarily small. That is, Q_r is not identically zero, whereas μ is assumed to be identically zero in assumption (a). Note that the apparent conflict between assumption (6) [page 12] requiring that $N_M = \mu_0 \sigma Q_r r$ be small and assumption (b) that σ be infinite is resolved in a practical situation by the requirement that $0 < Q_r < \epsilon$, since σ is always

finite, but can be sufficiently large (e.g., a liquid metal) as to be "effectively" infinite for purposes of the stability analysis.

A. Steady-State Solution

From Eq. (aa), Appendix I, with $h = 0$ and taking $J_r = J_0$ at $r = R$:

$$J_r = \frac{J_0 R}{r} . \quad (\text{ad})$$

This is the zeroth order approximation for J_r obtained on page 35.

The steady-state solution for Q_θ can now be found from Eq. (ad) and Eq. (l), Appendix I, with $\mu = 0$:

$$Q_r \frac{dQ_\theta}{dr} + \frac{Q_\theta Q_r}{r} = - \frac{J_0 R B_0}{r \rho} , \quad (\text{am})$$

$$Q_r = \frac{\text{const.}}{r} \quad [\text{see Eq. (j)}] . \quad (\text{aj})$$

The solution of Eqs. (am) and (aj) is:

$$Q_\theta = \frac{K}{r} + K' r , \quad (\text{an})$$

where

$$K' = \frac{\pi J_0 B_0 R}{m} ,$$

and

$$m \equiv -2\pi \rho Q_r r .$$

[Note that by assumption (d') $m \neq 0$, otherwise $Q_\theta \rightarrow \infty$ for $J_0 B_0 \neq 0$.]

For inviscid flow, the value of K is arbitrary. However, the non-slip condition at the outer wall, which is admitted by the general solution, is of the most practical interest, and gives

$$K = - \frac{\pi J_0 B_0 R^3}{m} .$$

B. Stability Criteria

The stability analysis employed by Chang will be closely followed here. Only those equations which are altered by virtue of assumption (c') and by the new steady-state solution for Q_θ [Eq. (an)] will be considered here; the reader must refer to ref. 8 for the intermediate equations and definitions of terms. Note that assumption (d') is equivalent to assumption (d) as far as the stability analysis is concerned, since Q_r is assumed so small that terms involving Q_r and its derivatives can be neglected.

The basic time dependent equations in cylindrical coordinates are Eqs. (2.12) through (2.19) of Chang's analysis, ref. 8. Small axisymmetric perturbations are assumed as follows:

$$q_r = \epsilon \tilde{q}_r, \quad (\text{ao})$$

$$q_\theta = \frac{K}{r} + K' r + \epsilon \tilde{q}_\theta, \quad (\text{ap})$$

$$q_z = \epsilon \tilde{q}_z, \quad (\text{aq})$$

$$B_r = \epsilon \tilde{B}_r, \quad (\text{ar})$$

$$B_\theta = \epsilon \tilde{B}_\theta, \quad (\text{as})$$

$$B_z = B_0 + \epsilon \tilde{B}_z, \quad (\text{at})$$

$$p^* = \left(P + \frac{B_0^2}{2 \mu_0} \right) + \epsilon \tilde{p}^*, \quad (\text{au})$$

$$\epsilon = \text{positive, real constant} \ll 1. \quad (\text{av})$$

An additional assumption is implied in Eq. (as):

$$\begin{aligned} \frac{\partial B_\theta}{\partial z} &= -\mu_0 J_r, \quad (\text{o}) \\ &= -\mu_0 \frac{J_0 R}{r}, \end{aligned}$$

$$\therefore B_\theta = -\mu_0 J_0 R \frac{z}{r} + f(r).$$

For B_θ to be negligible in the steady-state solution, it is sufficient that $f(r)$ be very small and that $\mu_0 J_0 R (z/r)$ likewise be very small (i.e., compared with B_0). If $f(r)$ is taken as zero so that $B_\theta = 0$ when $J_0 = 0$ (as assumed by Chang), then an additional restriction must be imposed:

$$(e) \quad \mu_0 J_0 R \frac{z}{r} \ll B_0 .$$

Chang's Eqs. (5.1), (5.2), and (5.3), (5.5), and (5.6) become for this case:

$$\frac{\partial \tilde{q}_r}{\partial t} + \left(\frac{K}{r^2} + K' \right) \frac{\partial \tilde{q}_r}{\partial \theta} - \left(\frac{2K}{r^2} + 2K' \right) \tilde{q}_\theta = \frac{B_0}{\rho \mu_0} \frac{\partial \tilde{B}_r}{\partial z} - \frac{1}{\rho} \frac{\partial \tilde{p}^*}{\partial r} , \quad (aw)$$

$$\frac{\partial \tilde{q}_\theta}{\partial t} + 2K' \tilde{q}_r + \left(\frac{K}{r^2} + K' \right) \frac{\partial \tilde{q}_\theta}{\partial \theta} = \frac{B_0}{\rho \mu_0} \frac{\partial \tilde{B}_\theta}{\partial z} , \quad (ax)$$

$$\frac{\partial \tilde{q}_z}{\partial t} + \left(\frac{K}{r^2} + K' \right) \frac{\partial \tilde{q}_z}{\partial \theta} = \frac{B_0}{\rho \mu_0} \frac{\partial \tilde{B}_z}{\partial z} - \frac{1}{\rho} \frac{\partial \tilde{p}^*}{\partial z} , \quad (ay)$$

$$\frac{\partial \tilde{B}_\theta}{\partial t} + \left(\frac{K}{r^2} + K' \right) \frac{\partial \tilde{B}_\theta}{\partial \theta} + \frac{2K}{r^2} \tilde{B}_r = B_0 \frac{\partial \tilde{q}_\theta}{\partial z} , \quad (az)$$

$$\frac{\partial \tilde{B}_z}{\partial t} + \left(\frac{K}{r^2} + K' \right) \frac{\partial \tilde{B}_z}{\partial \theta} = B_0 \frac{\partial \tilde{q}_z}{\partial z} . \quad (ba)$$

Equations (5.7) through (5.15) remain unchanged.

Equations (5.16), (5.17), and (5.20) become:

$$i a \hat{q}_r - \left(\frac{2K}{r^2} + 2K' \right) \hat{q}_\theta - \frac{i b B_0}{\rho \mu_0} \hat{B}_r + \frac{1}{\rho} \frac{d \hat{p}^*}{dr} = 0 , \quad (bb)$$

$$i a \hat{q}_\theta + 2K' \hat{q}_r - \frac{i b B_0 \hat{B}_\theta}{\rho \mu_0} = 0 , \quad (bc)$$

$$i a \hat{B}_\theta + \left(\frac{2K}{r^2} + 2K' \right) \hat{B}_r - i b B_0 \hat{q}_\theta = 0 . \quad (\text{bd})$$

Equations (5.18), (5.19), and (5.21) are unchanged.

Equations (6.1) and (6.3) are unchanged, but Eq. (6.2) becomes:

$$y_\theta = -\frac{i}{a} \left[\hat{q}_\theta + \frac{2i}{a} \left(\frac{K}{r^2} + K' \right) \hat{q}_r \right] . \quad (\text{be})$$

Equations (6.6) and (6.7) become:

$$\begin{aligned} -a^2 y_r - \left(\frac{2K}{r^2} + 2K' \right) \left[i a y_\theta + 2 \left(\frac{K}{r^2} + K' \right) y_r \right] - \\ - \frac{i b B_0}{\rho \mu_0} \hat{B}_r + \frac{1}{\rho} \frac{dp^*}{dr} = 0 , \end{aligned} \quad (\text{bf})$$

$$i a \left[i a y_\theta + 2 \left(\frac{K}{r^2} + 2K' \right) y_r \right] - \frac{i b B_0}{\rho \mu_0} \hat{B}_\theta = 0 . \quad (\text{bg})$$

Equation (6.8), Eqs. (6.12) through (6.15), and (6.18) are unchanged.

Equations (6.16) and (6.17) become:

$$\left[a^2 + 4 \left(\frac{K}{r^2} + K' \right)^2 - \frac{b^2 B_0^2}{\rho \mu_0} \right] y_r + 2i a \left(\frac{K}{r^2} + K' \right) y_\theta - \frac{1}{\rho} \frac{dp^*}{dr} = 0, (\text{bh})$$

$$- \left(a^2 - \frac{b^2 B_0^2}{\rho \mu_0} \right) y_\theta + 2i a \left(\frac{K}{r^2} + 2K' \right) y_r = 0 . \quad (\text{bi})$$

Eliminating y_θ , y_z , and p^* from Eqs. (6.15), (6.18), (bh), and (bi):

$$\begin{aligned} y_r \left\{ \left(a^2 - \frac{b^2 B_0^2}{\rho \mu_0} \right)^2 - 4 \left(\frac{K}{r^2} + K' \right) \left[\frac{b^2 B_0^2}{\rho \mu_0} \left(\frac{K}{r^2} + K' \right) + a^2 K' \right] \right\} = \\ = \frac{\left(a^2 - \frac{b^2 B_0^2}{\rho \mu_0} \right)^2}{b^2} \left(\frac{d^2 y_r}{dr^2} + \frac{1}{r} \frac{dy_r}{dr} - \frac{y_r}{r^2} \right) , \end{aligned} \quad (\text{bj})$$

which corresponds to Chang's Eq. (6.19); note the additional term multiplying y_r in this equation which does not appear in Eq. (6.19).

Omitting several of the intermediate steps, the equation for a^2 corresponding to Chang's Eq. (7.4) is:

$$\begin{aligned}
 a^2 = & \frac{b^2 B_0^2}{\rho \mu_0} + \left(\frac{2b^2 K' \int_e^R \left(\frac{K}{r^2} + K' \right) r y_r \bar{y}_r dr}{D'} \right) \pm \\
 & \pm \frac{1}{2} \left\{ \left[\frac{2b^2 B_0^2}{\rho \mu_0} + \frac{4b^2 K' \int_e^R \left(\frac{K}{r^2} + K' \right) r y_r \bar{y}_r dr}{D'} \right. \right. \\
 & \left. \left. - \frac{4b^4 B_0^4}{(\rho \mu_0)^2} + \frac{16b^4 B_0^2 \int_e^R \left(\frac{K}{r^2} + K' \right)^2 r y_r \bar{y}_r dr}{\rho \mu_0 D'} \right]^{1/2} \right. \quad (bk)
 \end{aligned}$$

where

$$D' \equiv b^2 \int_e^R r y_r \bar{y}_r dr - \int_e^R \frac{d}{dr} \left(\frac{dy_r}{dr} + \frac{y}{r} \right) r \bar{y}_r dr$$

The stability criterion is that a^2 be real and positive.

Following Chang's analysis, from Eqs. (8.1) through (8.5) and Eq. (8.15), noting assumption (d') [page 38 of this Appendix] which allows the boundary conditions expressed by Eqs. (8.3) and (8.4) to be used:

$$\begin{aligned}
 a^2 = & \left(\frac{b^2 B_0^2}{\rho \mu_0} + \frac{2b^2 K' \int_e^R \left(\frac{K}{r^2} + K' \right) r y_r^2 dr}{D} \right) \pm \\
 & \pm \frac{1}{2} \left\{ \left[\frac{2b^2 B_0^2}{\rho \mu_0} + \frac{4b^2 K' \int_e^R \left(\frac{K}{r^2} + K' \right) r y_r^2 dr}{D} \right]^2 \right. \\
 & \left. - \frac{4b^4 B_0^4}{(\rho \mu_0)^2} + \frac{16b^4 B_0^2 \int_e^R \left(\frac{K}{r^2} + K' \right)^2 r y_r^2 dr}{\rho \mu_0 D} \right]^{1/2} \right. \quad (bl)
 \end{aligned}$$

where

$$D \equiv \int_e^R r \left(\frac{dy_r}{dr} + \frac{y_r}{r} \right)^2 dr .$$

It can be shown from Eq. (bl) that a necessary condition for a^2 to be > 0 (after nondimensionalizing the integrals) is:

$$\frac{1}{A_e^2} = \frac{B_0^2}{\mu_0 \rho Q_e^2} \geq \frac{4\kappa^2}{(1 - \kappa^2)^2} \phi(\kappa) . \quad (\text{bm})$$

where

$$\phi(\kappa) \equiv \left\{ \frac{\int_{\kappa}^1 y_{r'}^2 \frac{(r'^2 - 1)^2 dr'}{r'^3}}{\int_{\kappa}^1 r' \left(\frac{dy_{r'}}{dr'} + \frac{y_{r'}}{r'} \right)^2 dr'} \right\} ,$$

using the definitions of K and K' given on page 39 and nondimensionalizing the integrals, and

$$A_e \equiv |Q_e| / \sqrt{B_0^2 / \rho \mu_0}$$

is the central Alfvén number, based on the tangential velocity, Q_e , at the inner radius, e :

$$Q_e \equiv - \frac{\pi J_0 B_0 R^2}{m} \left(\frac{1}{\kappa} - \kappa \right)$$

from Eq. (an) with $r' = \kappa$. Alternatively,

$$Q_e = - \frac{I_0 B_0 R}{20 m} \left(\frac{1 - \kappa^2}{\kappa} \right) . \quad (\text{bn})$$

Chang suggests the following form as an approximation for $y_{r'}$, as discussed on page 24 of ref. 8:

$$y_{r'} = y_{r'}^0 \sin \frac{\pi(r' - \kappa)}{(1 - \kappa)} \quad (\text{bo})$$

Using this function for $y_{r'}$ and restricting $\kappa \leq 0.7$, it can be shown that Eq. (bm) is both necessary and sufficient for $a^2 > 0$. Furthermore, for the special condition of equality in Eq. (bm), i.e.,

$$\frac{1}{A_e^2} = \frac{B_0^2}{\mu_0 \rho Q_e^2} = \frac{4\kappa^2}{(1 - \kappa^2)^2} \phi(\kappa) \quad (\text{bp})$$

the requirement that a^2 be real is also satisfied, although this is not a necessary requirement. Equation (bp) is used here as a sufficient criterion for stability, with the understanding that there may be other possible stable solutions which must be determined for each individual case from a more general analysis of the requirement that a^2 be real.

Solving Eq. (bp) explicitly for the magnetic field, B_0 :

$$\frac{B_0}{|Q_e|} = 2 \left(\frac{\kappa}{1 - \kappa^2} \right) \sqrt{\mu_0 \rho \phi(\kappa)} \quad (\text{bq})$$

By eliminating $|Q_e|$ between Eqs. (bn) and (bq), an alternate but equivalent formulation of the sufficient stability criterion is obtained:

$$\frac{I_0 R}{m} = \frac{10}{\sqrt{\mu_0 \rho \phi(\kappa)}} \quad (\text{br})$$

REFERENCES

1. Coleman DuP. Donaldson, "The Magnetohydrodynamic Vortex Power Generator - Basic Principles and Practical Problems," Aeronautical Research Associates of Princeton, Inc., ARAP Report No. 30, 1961.
2. W. S. Lewellan, "Magnetohydrodynamically Driven Vortices," pp. 1-13 in Heat Transfer and Fluid Mechanics Institute, Stanford University Press, Stanford, California (1960).
3. W. S. Lewellan and W. R. Grabowsky, "Nuclear Space Power Systems Using Magnetohydrodynamic Vortices," Am. Rocket Soc.: 693 (May 1962).
4. E. M. Knoernschild et al., "Vortex MHD Generator Design Study," AiResearch Mfg. Co., ASD Tech. Report 61-380 (November 1961).
5. J. L. Kerrebrock and R. V. Meghreblian, "Vortex Containment for the Gaseous Fission Rocket," J. Aerospace Sci., 28: 710-724 (1961).
6. R. J. Rosa, "Propulsion System Using a Cavity Reactor and MHD Generator," Am. Rocket Soc.: 884-889 (July 1961).
7. S. Chandrasekhar, Hydrodynamic and Hydromagnetic Stability, pp. 382-428, Clarendon Press, Oxford, 1961.
8. T. S. Chang, "Magnetohydrodynamic Stability of Vortex Flow - A Non-Dissipative, Incompressible Analysis," USAEC Report ORNL TM-402, Oak Ridge National Laboratory, October 23, 1962.
9. H. Görtler, "Über eine Dreidimensionale Instabilität Laminarer Grenzschichten an Konkaven Wänden," Nachr. Wiss. Ges., Göttingen, Math, Phys. Klasse, New Series, 2, No. 1 (1940).
10. J. J. Keyes, Jr., and R. E. Dial, "An Experimental Study of Vortex Flow for Application to Gas-Phase Fission Heating," USAEC Report ORNL-2837, Oak Ridge National Laboratory, April 16, 1960.
11. M. L. Rosenzweig, "Summary of Research in the Field of Advanced Nuclear Propulsion - January-June 1961," Space Technology Lab Report TDR-594(1203-01)STR.
12. J. T. Stuart, Proc. Royal Soc. (London), A 221: 189 (1956).
13. R. C. Lock, Proc. Royal Soc. (London), A 233: 105 (1955).
14. J. Hartmann and F. Lazarus, Kgl. Danske Videnskab, Mat.-fys. Medd., 15, Nos. 6 and 7 (1937).
15. W. Murgatroyd, Phil. Mag., 44: 1348 (1955).

16. Lawson P. Harris, Hydromagnetic Channel Flows, The Technology Press of The Massachusetts Institute of Technology and John Wiley and Sons, 1960.
17. R. J. Donnelly and M. Ozima, "Hydromagnetic Stability of Flow Between Rotating Cylinders," Phys. Rev. Letters, 4: 497-498 (1960).
18. L. R. Boedeker and E. E. Covert, "Measurements of Helical Flow of a Strong Electrolyte with and without a Transverse Magnetic Field," MIT Aerophysics Laboratory Report AFOSR 2806, April 1962.
19. J. J. Keyes, Jr., "An Experimental Study of Flow and Separation in Vortex Tubes with Application to Gaseous Fission Heating," Am. Rocket Soc.: 1204 (September 1961).
20. R. E. English et al., "A 20,000-Kilowatt Nuclear Turboelectric Power Supply for Manned Space Vehicles," NASA Memo 2-20-59 E, March 1959.
21. T. S. Chang, "Introduction to Magneto-Fluid Mechanics," USAEC Report ORNL TM-436, Oak Ridge National Laboratory, December 17, 1962.

NOMENCLATURE

A_e	central Alfvén modulus, $ Q_e /\sqrt{B_0^2/\rho \mu_0}$
A_p	peripheral Alfvén modulus, $Q_p/\sqrt{B_0^2/\rho \mu_0}$
a	number of valence electrons per atom
B	magnetic induction field, gauss
B_0	applied axial magnetic field, gauss
\tilde{B}	perturbation component of magnetic induction field, gauss
Λ_B	normal mode amplitude of magnetic induction field, gauss
b	convective wave number, cm^{-1}
E	electric field intensity, emu/cm
e	inner radius of vortex field, cm
e'	electronic charge, emu
H'	Hall effect parameter defined by Eq. (ag), Appendix I
h	Hall coefficient, cm^3/emu
I_0	applied electric current per unit length, amp/cm
J	electric current density, emu/cm^2
J_0	applied electric current density at circumference of vortex tube, emu/cm^2
K	$-\frac{\pi J_0 B_0 R^3}{m}$
K_1, K_2, K_3	constants defined by Eqs. (aj), (ak), and (al)
K'	$\frac{\pi J_0 B_0 R}{m}$
L	effective shearing length in Eq. (6), cm
M	tangential Mach number
m	mass flow per unit length, $\text{g/sec}\cdot\text{cm}$

N	radial Reynolds modulus, $-m/2\pi \mu$
N_H	Hartmann modulus, defined by Eq. (6)
N_M	radial magnetic Reynolds modulus, $\mu_0 \sigma Q_r r$
n	valence electron density, cm^{-3}
P	mean (time average) pressure, dyne/cm^2
p	fluid pressure, dyne/cm^2
p^*	equivalent fluid pressure, dyne/cm^2
\tilde{p}^*	perturbation of the equivalent fluid pressure, dyne/cm^2
\hat{p}^*	normal mode amplitude of the perturbation component of the fluid pressure, dyne/cm^2
Q	mean (time average) velocity, cm/sec
Q_e	mean tangential velocity at inner radius of vortex flow field, cm/sec
Q_p	mean tangential velocity at outer radius of vortex flow field, cm/sec
q	instantaneous velocity, cm/sec
\tilde{q}	perturbation component of the velocity, cm/sec
\hat{q}	normal mode amplitude of the component of fluid velocity, cm/sec
R	radius of outer boundary, cm
r	radial distance, cm
r'	relative radius, r/R
t	time, sec
V	applied emf, volt
W	atomic weight, g/g atom
y	transformed functions related to the amplitude functions \hat{q} (see ref. 8)
\bar{y}	complex conjugate of y
y^0	amplitude of the approximate eigenfunction y_r for stability (see ref. 8)
z	axial distance, cm

Greek Letters

- $\beta(\kappa)$ function defined by Eq. (3)
- ϵ positive, real infinitesimal
- ϵ_{ijk} permutation symbol in index notation
- κ ratio of inner to outer radius of vortex flow field, e/R
- μ viscosity, $g/cm \cdot sec$
- μ_0 magnetic permeability ($= 4\pi$ in cgs-emu units)
- ρ density, g/cm^3
- σ electrical conductivity, emu/cm
- σ' effective (Hall) electrical conductivity, emu/cm
- $\phi(\kappa)$ function defined in Eq. (bm)

Subscripts

- e value at vortex inner radius
- i, j, k index notation suffixes
- p value at vortex outer radius
- r radial coordinate component
- z axial coordinate component
- θ circumferential coordinate component

INTERNAL DISTRIBUTION

1. S. E. Beall
2. M. Bender
3. A. L. Boch
4. R. B. Briggs
5. R. D. Bundy
6. J. W. Cooke
7. R. E. Dial
8. D. M. Eissenberg
9. A. P. Fraas
10. W. R. Gambill
11. W. F. Gauster
12. B. L. Greenstreet
- 13-14. H. W. Hoffman
- 15-24. J. J. Keyes, Jr.
25. G. J. Kidd, Jr.
26. A. I. Krakoviak
27. C. G. Lawson
28. R. N. Lyon
29. H. G. MacPherson
30. W. D. Manly
31. A. J. Miller
32. A. M. Perry
33. M. W. Rosenthal
34. W. K. Sartory
35. H. W. Savage
36. A. W. Savolainen
37. E. D. Shipley
38. M. J. Skinner
39. I. Spiewak
40. J. A. Swartout
41. D. G. Thomas
42. D. B. Trauger
43. J. L. Wantland
44. R. P. Wichner
- 45-46. Central Research Library (CRL)
- 47-49. Y-12 Document Reference Section (DRS)
- 50-55. Laboratory Records Department (LRD)
56. Laboratory Records Department - Record Copy (LRD-RC)
57. Reactor Division Library, Bldg. 9204-1

EXTERNAL DISTRIBUTION

- 58-72. Division of Technical Information Extension (DTIE)
73. Research and Development Division, ORO
- 74-75. Reactor Division (ORO)

